sciendo
Control and Cybernetics
vol. **50** (2021) No. 3
pages: 263-301
DOI: 10.2478/candc-2021-0019

Pre-shape calculus and its application to mesh quality optimization*

by

Daniel Luft and Volker Schulz

Trier University, Department of Mathematics, 54286 Trier, Germany
luft@uni-trier.de
volker.schulz@uni-trier.de

Abstract: Deformations of the computational mesh, arising from optimization routines, usually lead to decrease of mesh quality or even destruction of the mesh. We propose a theoretical framework using pre-shapes to generalize the classical shape optimization and calculus. We define pre-shape derivatives and derive corresponding structure and calculus theorems. In particular, tangential directions are featured in pre-shape derivatives, in contrast to classical shape derivatives, featuring only normal directions. Techniques from classical shape optimization and calculus are shown to carry over to this framework. An optimization problem class for mesh quality is introduced, which is solvable with the use of pre-shape derivatives. This class allows for simultaneous optimization of the classical shape objectives and mesh quality without deteriorating the classical shape optimization solution. The new techniques are implemented and numerically tested for 2D and 3D.

Keywords: shape optimization, mesh quality, mesh deformation method, shape calculus

1. Introduction

1.1. The subject of the paper

Solutions of PDE constrained optimization problems, in particular – problems where the desired control variable is a geometric shape, are only meaningful, if the state variables of the constraint can be calculated with sufficient reliability. A key component of reliable solutions is given by the quality of the computational mesh. It is well-known that poor quality of elements affect the stability, convergence, and accuracy of finite element and other solvers.

*Submitted: April 2021; Accepted: June 2021.

We propose a unified framework, using the so-called pre-shapes. In this setting, both shape optimization and mesh quality optimization problems can be formulated at the same time. We give a class of problems called pre-shape parameterization tracking problems, which can act as regularizations for shape optimization problems. These problems can be solved for volume and surface meshes with arbitrary dimension, and yield numerical algorithms similar to so called mesh deformation methods, which reallocate nodes of numerical meshes according to targeted element volumes in order to improve mesh quality. At the same time, the proposed framework is suitable to derive a calculus mimicking classical shape calculus. This enables formulation of efficient routines solving shape optimization problems, which, at the same time, optimize quality of the surface mesh, representing the shape, without noticeable additional computational cost or interference with the original shape optimization problem. With this, the desired surface and the surrounding volume mesh quality are ensured during shape optimization.

In this paper we will establish the theoretical foundations of pre-shape optimization and calculus, and show its connection to classical shape calculus. We implement these methods in the form of a pre-shape gradient descent to achieve a targeted quality of volume and surface meshes without a shape optimization target. In Luft and Schulz (2021), we build on the achievements of this paper, and introduce theoretical and numerical results to solve shape optimization problems while simultaneously improving volume and shape mesh quality according to targeted node distributions. The techniques, elaborated in Luft and Schulz (2021) leave optimal shapes invariant and offer minimal additional numerical costs. They also permit the use of different metrics to represent gradients. We compare pre-shape mesh regularizations for various metrics in Luft and Schulz (2021) for a hard to solve shape optimization problem.

1.2. Literature review

We give a brief overview of techniques related to the ones treated in this article. Our methods are not related to mesh untangling and -relaxation, edge swapping or remeshing strategies, such as those in Freitag (1997), Frey and Borouchaki (1999), Algorri and Schmitt (1996), Johnson, Sullivan and Kwasnick (1991). Of course, as there is a vast amount of literature concerning mesh generation and improvement strategies thereof, we can only give a selective overview. Two very prominent classes of techniques for mesh quality improvement are the so called mesh deformation method and methods based on Laplacian smoothing. Mesh deformation methods go back to a theoretical result, initially proposed by Moser (1965), extended by Banyaga (1974) and by Dacorogna and Moser (1990). This gave rise to mesh deformation methods pioneered by Liao and Anderson (1992), which redistribute mesh vertices so that uniform cell volumes are achieved. Mesh deformation methods are powerful, because they prevent mesh tangling while offering precise control over the element volumes. The

original method was further developed in various directions by Liao and associates (see Bochev, Liao and dela Pena, 1996; Liu, Ji and Liao, 1998; Cai, Jiang and Liao, 2004; Zhou, Chen and Liao, 2017). These advances allow to target non-uniform cell volume distributions, make deformation methods applicable to time-dependent problems, and show its use in higher order mesh generation methods. Also, the combination of multigrid- and mesh deformation methods was analyzed and implemented by Turek and associates (see Wan and Turek, 2006; Grajewski, Köster and Turek, 2009, 2010). A different family of mesh quality improvement techniques are those based on Laplacian smoothing (Field, 1988; Freitag, 1997; Shontz and Vavasis, 2003; Zhang, Bajaj and Xu, 2009). They do not necessarily track for cell volume distributions, but, instead, improve quality by averaging or smoothing vertex coordinates more or less specifically. Several strategies for increasing mesh quality, not based on mesh deformation methods mentioned or Laplacian smoothing, exist. In the context of shape optimization and -morphing, these include correcting for errors, frequently arising in discretizations of Hadamard's theorem (Etling et al., 2018), adding non-linear advection terms in shape gradient representations (Onyshkevych and Siebenborn, 2020), approximating shape morphing by volume-preserving mean-curvature flows (Laurain and Walker, 2020), and use of techniques related to centroidal Voronoi reparameterization in combination with eikonal equation based non-linear advection terms for representation of shape gradients (Schmidt, 2014).

2. General theory for pre-shape calculus

2.1. Pre-shape spaces

In order to provide theoretical grounds for the numerical procedures we are about to elaborate in the subsequent paper, we need to specify a framework for the objects, 'shapes', with respect to which we seek to optimize. Several possible theories and techniques exist in order to precisely formulate the notion of shapes. For example, shapes can be viewed as sets together with corresponding characteristic functions in an ambient space, leading to an approach which emphasizes geometric measure theory as in Delfour and Zolésio (2001). We choose a different setting, namely a shape space approach using infinite dimensional differential geometry, since it naturally permits to view the shape and its parameterization at the same time. This is the key to extending numerical routines in a way that optimizes parameterizations, i.e. meshes, in a desired way without interfering with the shape optimization taking place. For an excellent overview of shape spaces we refer to Bauer, Bruveris and Michor (2014), from which we borrow several definitions for the following introduction to shape spaces considered in this article.

For the rest of this article, let M be an n-dimensional, orientable, path-connected and compact $C^{k,\alpha}$- or C^∞-manifold. Further, we will use $\mathbb{R}^{n+1}$ as the

ambient space for building our theory. In particular only shapes of codimension 1 are considered.

Denote by $\mathrm{Diff}(M)$ the regular Lie-group of C^∞-diffeomorphisms of M onto itself. Then, the space B_e of unparameterized C^∞-shapes in $\mathbb{R}^{n+1}$ is defined by (see Michor and Mumford, 2005)

$$B_e(M, \mathbb{R}^{n+1}) := \mathrm{Emb}(M, \mathbb{R}^{n+1}) / \mathrm{Diff}(M), \tag{1}$$

where $\mathrm{Emb}(M, \mathbb{R}^{n+1})$ is the space of all C^∞-embeddings of M into $\mathbb{R}^{n+1}$ and $\mathrm{Diff}(M)$ is acting on the right. For avoidance of confusion, we remember that in this context a C^∞-embedding is an injective, smooth map $\varphi : M \to \mathbb{R}^{n+1}$, which has injective first derivative everywhere, i.e. φ is an injective immersion. The resulting space $B_e(M, \mathbb{R}^{n+1})$, is also called non-linear Grassmannian (see Kriegl and Michor, 1997) or differentiable Chow-variety. It forms a smooth Hausdorff manifold, whose elements can be regarded as unparameterized hypersurfaces of $\mathbb{R}^{n+1}$ (see Michor and Mumford, 2007, Corollary 3.3). In the following we will abbreviate $B_e(M, \mathbb{R}^{n+1})$ by B_e^n, still having the implicit relation to the manifold M and its dimension in mind. This space can be equipped with various metrics, which means shape optimization can be regarded as optimization on an infinite dimensional Riemannian manifold (see Schulz, 2014). Notice that B_e^n is not a manifold if C^∞-regularity is replaced by Hölder- or Sobolev-regularity. In this more general setting, resulting spaces have a diffeological structure (see Welker, 2017). To acquire intuition, a graphical visualization of B_e^n is given in Fig. 1.

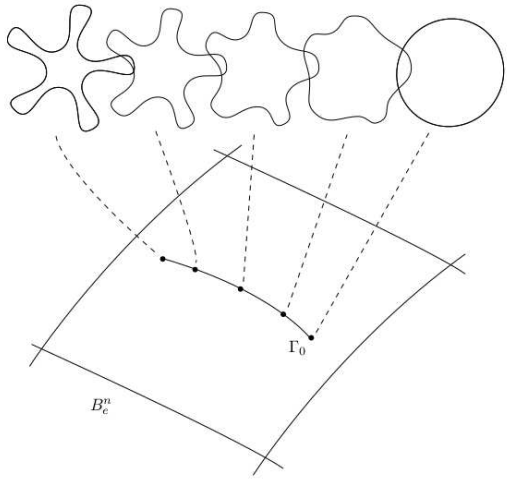

Figure 1: Illustration of a path in the shape space B_e^n for $M = S^1$

For our purposes it is not enough to view shape optimization as optimization in B_e^n. Instead, we will exploit additional structures on the space $\mathrm{Emb}(M, \mathbb{R}^{n+1})$

induced by the action of $\mathrm{Diff}(M)$ and base our framework as optimization in $\mathrm{Emb}(M, \mathbb{R}^{n+1})$. Elements $\varphi \in \mathrm{Emb}(M, \mathbb{R}^{n+1})$ can be interpreted as parameterized shapes in the ambient space $\mathbb{R}^{n+1}$, whereas elements of $\mathrm{Diff}(M)$, acting on the right, can be seen as reparameterizations. The authors of Bauer, Bruveris and Michor (2014, Chapter 1.1) call $\mathrm{Emb}(M, \mathbb{R}^{n+1})$ *pre-shape space*, an expression we will borrow for the techniques we will build in this paper. Notice that the term *pre-shape space* is used differently, depending on the literature, e.g. in Kendall et al. (2009), where the authors use this term for the space of labeled landmarks, which are equivalent under translation and scaling.

The additional structure of parameterized shapes $\varphi \in \mathrm{Emb}(M, \mathbb{R}^{n+1})$, compared to unparameterized shapes $\Gamma \in B_e^n$, enables to not just view the shape itself, but also to distinguish various types of discretizations in the ambient space and the corresponding numerical meshes. Even further, this concept enables to control the parameterization of the hold-all domain itself, allowing for control of the way volume meshes are discretized. The structure for this is given by the fact (see Kriegl and Michor, 1997, Theorem 44.1; Binz and Fischer, 1981) that the quotient map

$$\pi : \mathrm{Emb}(M, \mathbb{R}^{n+1}) \to B_e(M, \mathbb{R}^{n+1}) \tag{2}$$

makes $\mathrm{Emb}(M, \mathbb{R}^{n+1})$ the *total space of the smooth principal fibration* with $\mathrm{Diff}(M)$ acting as the *structure group* or *standard fiber*, B_e^n being the *base space*, which goes back to Binz and Fischer (1981). As a reminder, a fiber bundle is a manifold, which locally looks like a product space $B \times F$, where B corresponds to the base space, and F corresponds to the standard fiber. In our context, this means that the pre-shape space $\mathrm{Emb}(M, \mathbb{R}^{n+1})$ is the collection of parameterized shapes, which locally looks like 'Shape'×'Parameterization'. However, this relationship holds only locally, and the global structure of the pre-shape space $\mathrm{Emb}(M, \mathbb{R}^{n+1})$ is much more complex. The situation is graphically sketched in Fig. 2.

An application of the bundle projection π to a parameterized shape $\varphi \in \mathrm{Emb}(M, \mathbb{R}^{n+1})$ results in its unparameterized shape $\pi(\varphi) \in B_e^n$ in the base space. Hence, we can view the fiber $\pi(\varphi)$ as the collection of all parameterizations of the shape $\varphi(M)$. It is important to avoid confusion of $\varphi(M)$ and $\pi(\varphi)$, which are both called shapes. The first interprets shapes as *subsets* $\varphi(M) \subset \mathbb{R}^{n+1}$, the latter as *equivalence-classes*, i.e.

$$\pi(\varphi) := \{\psi \in \mathrm{Emb}(M, \mathbb{R}^{n+1}) : \ \exists \rho \in \mathrm{Diff}(M) \ s.t. \ \varphi = \psi \circ \rho\} \in B_e^n. \tag{3}$$

The equivalence class interpretation is the collection of parameterizations corresponding to a certain shape in $\mathbb{R}^{n+1}$.

In order to formulate an analogue of shape calculus in $\mathrm{Emb}(M, \mathbb{R}^{n+1})$, we need to characterize the tangential bundles $T\,\mathrm{Emb}(M, \mathbb{R}^{n+1})$ and TB_e^n, as well as their relations. For this, we make use of results by Kriegl and Michor (1997).

Since we assume M to be compact, the respective tangent bundle of the pre-shape space is isomorphically given by

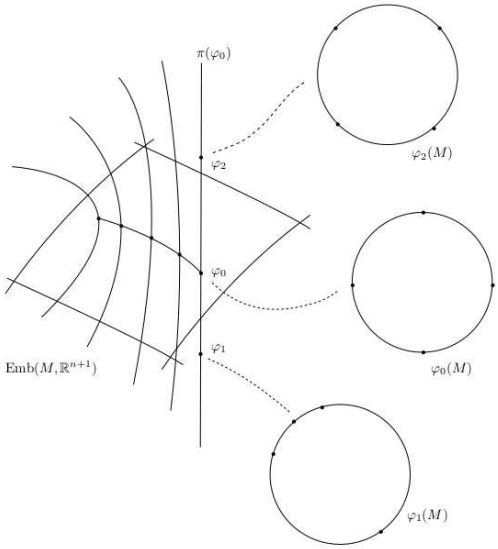

Figure 2: Illustration of the pre-shape space $\mathrm{Emb}(M,\mathbb{R}^{n+1})$ for $M = S^1$. To illustrate the parameterization interpretation of fibers $\pi(\varphi)$, the same four points are mapped from M to $\varphi_i(M)$

$$T_\varphi \mathrm{Emb}(M,\mathbb{R}^{n+1}) \cong C^\infty(\varphi(M),\mathbb{R}^{n+1}) \quad \forall \varphi \in \mathrm{Emb}(M,\mathbb{R}^{n+1}). \tag{4}$$

The fiber-bundle structure leads to a decomposition of the tangent bundle of the total space $T\,\mathrm{Emb}(M,\mathbb{R}^{n+1})$ into the so called *vertical bundle*, defined as $\ker T\pi \subset T\,\mathrm{Emb}(M,\mathbb{R}^{n+1})$, and the *horizontal bundle*. Since we only deal with compact and orientable n-dimensional manifolds M, the existence of outer normal vector-fields n on $\varphi(M) \subset \mathbb{R}^{n+1}$ is guaranteed. In the following, let $\langle .,. \rangle_2$ denote the L^2-scalar product. Thus, we obtain

$$T_\varphi \mathrm{Emb}(M,\mathbb{R}^{n+1}) \cong \mathcal{T}_{\varphi(M)} \oplus \mathcal{N}_{\varphi(M)} \quad \forall \varphi \in \mathrm{Emb}(M,\mathbb{R}^{n+1}), \tag{5}$$

where

$$\mathcal{T}_{\varphi(M)} := \{h \in C^\infty(\varphi(M),\mathbb{R}^{n+1}) : \langle h, n\rangle_2 = 0 \ \text{ on } \varphi(M)\} \tag{6}$$

is the *space of tangential vector fields on* $\varphi(M)$ in the ambient space $\mathbb{R}^{n+1}$, with

$$\mathcal{N}_{\varphi(M)} := \{h \in C^\infty(\varphi(M),\mathbb{R}^{n+1}) : h = \alpha \cdot n, \ \alpha \in C^\infty(\varphi(M),\mathbb{R})\} \tag{7}$$

being the *space of normal vector fields on* $\varphi(M)$. The tangential fields are parts of the vertical bundle, whereas the normal fields constitute the horizontal bundle

part. This also gives the well-known characterization of the tangential bundle of the classical shape space B_e^n via normal vector fields, i.e.

$$T_{\pi(\varphi)}B_e^n \cong \mathcal{N}_{\varphi(M)} \cong C^\infty(\varphi(M), \mathbb{R}) \quad \forall \pi(\varphi) \in B_e^n. \tag{8}$$

As previously, we also visualize the situation for tangential bundles in respective figures, namely Figs. 3 and 4.

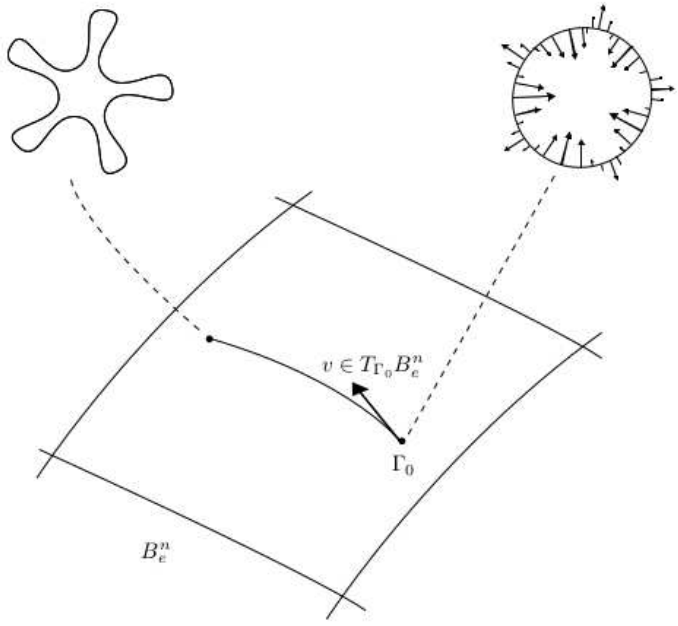

Figure 3: Illustration of a shape tangential vector from TB_e^n for $M = S^1$

2.2. Pre-shape calculus

Next, we introduce a suitable notion of objective functionals. We are inspired by Delfour and Zolésio (2001, Chapter 4.3.1), where shape functionals $\mathcal{J}$ are functions on a set of admissible shapes $\mathcal{A}$, which are considered to be a subset of the power set $\mathcal{A} \subseteq \mathcal{P}(\mathbb{R}^{n+1})$. This is a set-theoretic approach, because the power set $\mathcal{P}(\mathbb{R}^{n+1})$ is the set of all subsets of $\mathbb{R}^{n+1}$. Since we can canonically associate every equivalence class $\pi(\varphi) \in B_e^n$ with its set $\varphi(M) \subset \mathbb{R}^{n+1}$, we get the following definition for the special set of admissible shapes B_e^n.

Definition 1 (Shape and Pre-Shape Functionals) *Let M be an n-dimensional, orientable, path-connected and compact C^∞-manifold. Consider the*

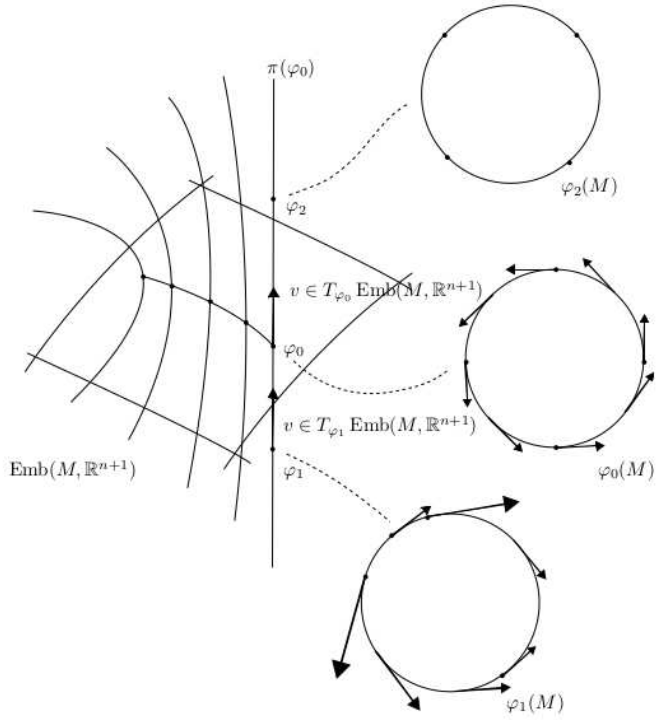

Figure 4: Illustration of vectors from $T \operatorname{Emb}(M, \mathbb{R}^{n+1})$ with pure tangential/vertical components for $M = S^1$. Note that four points are added to illustrate the parameterization interpretation of fibers $\pi(\varphi)$

shape space B_e^n *as defined in eq.* (1) *and the space of embeddings* $\operatorname{Emb}(M, \mathbb{R}^{n+1})$*. Then, a function*

$$\mathcal{J} : B_e^n \to \mathbb{R} \tag{9}$$

is called shape functional*, and a function*

$$\mathfrak{J} : \operatorname{Emb}(M, \mathbb{R}^{n+1}) \to \mathbb{R} \tag{10}$$

is called pre-shape functional*.*

The nomenclature of *pre-shape functional* for functions as in eq. (10) is motivated by regarding $\operatorname{Emb}(M, \mathbb{R}^{n+1})$ as a pre-shape space, like in Bauer, Bruveris and Michor (2014, Chapter 1.1). Since optimization is classically taking place in shape spaces as opposed to pre-shape spaces, we will highlight some of their correspondences and relations. The following definition is motivated by the construction of the shape space B_e^n in eq. (1).

Definition 2 (Shape Functionality) *Let $\mathfrak{J}$ be a pre-shape functional and let $\varphi \in \mathrm{Emb}(M, \mathbb{R}^{n+1})$. We say that $\mathfrak{J}$ has* shape functionality in φ *if it is consistent with the fiber projection, i.e.*

$$\mathfrak{J}(\varphi \circ \rho) = \mathfrak{J}(\varphi) \quad \forall \rho \in \mathrm{Diff}(M). \tag{11}$$

If $\mathfrak{J}$ has shape functionality for all $\varphi \in \mathrm{Emb}(M, \mathbb{R}^{n+1})$, we say that $\mathfrak{J}$ has shape functionality.

In order to give optimality criteria for the pre-shape optimization problems and to formulate the derivative based optimization algorithms, we need to introduce a shape derivative analogue for $\mathrm{Emb}(M, \mathbb{R}^{n+1})$. Also, it is desirable that the analogue be compatible with the classical Eulerian derivative, as, for example, found in Delfour and Zolesio (2001, Chapter 4.3.2) or in Schulz, Siebenborn and Welker (2016, Chapter 2.1). This motivates us to proceed in the fashion of classical shape optimization by defining a *pre-shape derivatives* based on families of deformations perturbing the image space. We show their relation to classical shape derivatives, and then give a structure theorem, similar to the Hadamard-Zolésio structure theorem (see Delfour and Zolésio, 2001, Chapter 9, Theorem. 3.6). Shape calculus or sensitivity analysis of classical shape optimization (see Haslinger and Mäkinen, 2003, Chapter 3; Berggren, 2010) will carry over to pre-shape spaces naturally.

Remark 1 (Validity of pre-shape theory for different regularities of shapes) *We want to remind the reader that the choice of C^∞-regularity for pre-shapes in $\mathrm{Emb}(M, \mathbb{R}^{n+1})$ is not necessary to introduce the concepts of this section, but merely serves as an exemplary situation. It is clear that the same definitions apply for embeddings φ of Sobolev- or Hölder-regularity. In these cases test functions and directions V need of course to have corresponding regularity.*

Definition 3 (Perturbation of Identity and Pre-shape Derivatives) *Let $\mathfrak{J}$ be a pre-shape functional (not necessarily having shape functionality), $\varphi \in \mathrm{Emb}(M, \mathbb{R}^{n+1})$ and $V \in C^\infty(\mathbb{R}^{n+1}, \mathbb{R}^{n+1})$. Then, the family of functions*

$$\varphi_t := \varphi + t \cdot V \circ \varphi \tag{12}$$

is called perturbation of identity of φ in direction V *for $t \in [0, \tau)$ and some $\tau > 0$. The limit*

$$\mathfrak{D}\mathfrak{J}(\varphi)[V] := \lim_{t \downarrow 0} \frac{\mathfrak{J}(\varphi_t) - \mathfrak{J}(\varphi)}{t} \tag{13}$$

is called pre-shape derivative *for $\mathfrak{J}$ at $\varphi \in \mathrm{Emb}(M, \mathbb{R}^{n+1})$ in direction V, if it exists and is linear and bounded in V.*

The perturbation of identity for shapes at $\Gamma_0 \subset \mathbb{R}^{n+1}$ in direction $V \in C^\infty(\mathbb{R}^{n+1}, \mathbb{R}^{n+1})$ is defined by

$$\Gamma_t := \{x_0 + t \cdot V(x_0) : x_0 \in \Gamma_0\}. \tag{14}$$

Notice that this is a set, in contrast to the perturbation of identity for pre-shapes, eq. (12), which is a function in $\mathrm{Emb}(M, \mathbb{R}^{n+1})$. Shape derivatives of a shape functional $\mathcal{J}$ are given by

$$\mathcal{D}\mathcal{J}(\Gamma_0)[V] := \lim_{t \downarrow 0} \frac{\mathcal{J}(\Gamma_t) - \mathcal{J}(\Gamma_0)}{t}. \tag{15}$$

The difference quotients, defining pre-shape and shape derivatives use completely different objects, therefore their difference is significant. Their relationship is explored in Proposition 1 and Theorem 1 further on.

The proposition below shows a result relating shape differentiability of classical shape optimization and pre-shape derivatives.

Proposition 1 (Shape Differentiability implies Pre-Shape Differentiability) *Consider a shape functional $\mathcal{J} : B_e^n \to \mathbb{R}$. Then it has a canonical extension to a pre-shape functional*

$$\mathfrak{J} : \mathrm{Emb}(M, \mathbb{R}^{n+1}) \to \mathbb{R},\ \varphi \mapsto \mathcal{J}(\pi(\varphi)), \tag{16}$$

where π is the bundle projection as in eq. (2). Further, there is a one-to-one correspondence of shape functionals $\mathcal{J}$ and pre-shape functionals $\mathfrak{J}$ with the property of shape functionality. Additionally, if $\mathcal{J}$ is shape differentiable in the classical sense, then its extension $\mathfrak{J}$ is pre-shape differentiable.

Proof One-to-one correspondence of pre-shape functionals with the property of shape functionality as in Definition 2 and classical shape functionals as in eq. (9) is clear. On the one hand, every canonical extension, eq. (16), of a classical shape functional $\mathcal{J}$ has shape functionality. On the other hand, every pre-shape functional $\tilde{\mathfrak{J}}$ having shape functionality gives rise to a shape functional $\mathcal{J}$ fulfilling eq. (16), as every fiber $\pi(\varphi)$ is the orbit of a φ by $\mathrm{Diff}(M)$ acting from the right.

The pre-shape differentiability assertion in Propositon 1 holds, since $\mathcal{J} \circ \pi$ extends the values of $\mathcal{J}$ constantly onto the fibers of $\mathrm{Emb}(M, \mathbb{R}^{n+1})$. For a fixed $\varphi \in \mathrm{Emb}(M, \mathbb{R}^{n+1})$, a case analysis for directions $V \in C^\infty(\mathbb{R}^{n+1}, \mathbb{R}^{n+1})$ being either tangential or normal at $\varphi(M)$ can be made. In case of horizontal, i.e. normal, directions V we recover the classical shape derivative $\mathcal{D}\mathcal{J}$. On the other hand, the pre-shape derivative in vertical directions can be represented as a differential via curves on $\varphi(M)$, which, combined with $\mathcal{J} \circ \pi$ extending $\mathcal{J}$ constantly on fibers, gives a vanishing pre-shape derivative. Linearity and boundedness of $\mathfrak{D}(\mathcal{J} \circ \pi)(\varphi)[V]$ in V are easy to see due to its vanishing for tangential components of V, together with linearity and boundedness of the classical shape derivative $\mathcal{D}\mathcal{J}$ by assumption. □

We can now situate the classical shape optimization problems in the context of optimization in pre-shape spaces $\mathrm{Emb}(M, \mathbb{R}^{n+1})$ for suitable manifolds M. But first, we observe that a unique solution $\varphi(M)$ of a shape optimization problem has multiple parameterizations in general. For shape optimization problems posed in the pre-shape space $\mathrm{Emb}(M, \mathbb{R}^{n+1})$, this leads to non-uniqueness

of solutions, which might at first appear like a disadvantage. However, due to non-uniqueness up to elements in the solution fiber $\pi(\varphi)$, it is possible to demand additional properties for the pre-shape solution. This gives several opportunities for enhancing numerical shape optimization routines, while at the same time narrowing down the amount of non-uniqueness of pre-shape solutions to a reasonable level. We will exploit this in upcoming works, such as Luft and Schulz (2021), where we increase mesh quality in shape optimization problems. Proposition 1 also offers a possibility to transfer results, concerning shape differentiability of classical shape functionals, to the pre-shape setting without the need for new proofs. In particular, existence of stationary points in B_e^n is carried over to $\mathrm{Emb}(M, \mathbb{R}^{n+1})$ as existence of stationary fibers. Hence, Proposition 1 shows that pre-shape optimization is in some sense a canonical generalization to classical shape optimization.

The definition of material- and shape derivatives found in classical shape optimization and structural sensitivity analysis literature (see Beggren, 2010, Definitions 1 and 2; Haslinger and Mäkinen, 2003, Chapter 3.3.1), possesses useful properties for practical applications. In particular, through the use of material derivatives, it is often straightforward to derive expressions for shape derivatives of integral quantities. We proceed by extending the notion of material derivatives from the classical context to the pre-shape calculus framework in order to harness these practical benefits.

Definition 4 (Pre-Shape Material Derivative) *Consider a family of functions* $\{f_\varphi : \mathbb{R}^{n+1} \to \mathbb{R}\}_{\varphi \in \mathrm{Emb}(M, \mathbb{R}^{n+1})}$. *For a direction* $V \in C^\infty(\mathbb{R}^{n+1}, \mathbb{R}^{n+1})$, *we define the* pre-shape material derivative *in* $x_0 \in \mathbb{R}^{n+1}$ *by*

$$\mathfrak{D}_m f(\varphi)[V](x_0) := \frac{\mathrm{d}}{\mathrm{d}t}_{|t=0} f_{\varphi_t}(x_t), \tag{17}$$

if the limit exists. Here, φ_t *is the perturbation of identity for pre-shapes (cf. eg. (12)) and* $x_t = x_0 + t \cdot V(x_0)$ *is a perturbed point.*

A careful reader might notice the similarity of classical shape and pre-shape material derivatives. The main difference is a possible dependence of functions f on parameterizations of shapes/domains they are defined for. Still, both notions coincide if the pre-shape functional has shape functionality, as we will see in Corollary 1 coming from the main Structure Theorem 1.

The definition of the material derivative can be generalized to functions and domains of weaker regularity, such as Sobolev functions and open subset $\Omega \subset \mathbb{R}^{n+1}$ with Lipschitz boundaries. A necessity for this comes from the fact that state solutions stemming from PDE constrained shape optimization problems need a well-defined material derivative for sensitivity analysis to be convenient. This is done in the same way as with the classical shape material derivative (see Haslinger and Mäkinen, 2009, p. 111).

It is further important to notice that the family f_φ can be seen as a function $f : \mathrm{Emb}(M, \mathbb{R}^{n+1}) \times \mathbb{R}^{n+1} \to \mathbb{R}$. In the first component, the perturbation of

identity for pre-shapes comes into play, which differs from the classical shape-material derivative. This leads to the following decomposition of the material derivative, which is similar to classical shape calculus, e.g. given by Haslinger and Mäkinen (2003, p. 111, (3.39),

$$\mathfrak{D}_m f(\varphi)[V] = \mathfrak{D} f(\varphi)[V] + \nabla f_\varphi^T V. \tag{18}$$

In the following we give a characterization of the pre-shape derivative in the style of the Hadamard-Zolésio structure theorem as found in Delfour and Zolésio (2001, Chapter 9, Theorem 3.6). For explanations, concerning the use of distributions, as we do in the following, the reader can consult Rudin (1991, Remark 6.2, Defitions. 6.22, 6.34, Theorem 7.10, Example 7.12).

Theorem 1 (Structure Theorem for Pre-Shape Derivatives)
Let $\mathfrak{J} : \mathrm{Emb}(M, \mathbb{R}^{n+1}) \to \mathbb{R}$ be a pre-shape differentiable pre-shape functional (not necessarily having shape functionality) and let $\varphi \in \mathrm{Emb}(M, \mathbb{R}^{n+1})$. Denote by $n_{\varphi(M)}$ the outer normal vector field of a shape $\varphi(M)$ for a $\varphi \in \mathrm{Emb}(M, \mathbb{R}^{n+1})$.

Then, the following holds:

(i) The support of $\mathfrak{D}\mathfrak{J}(\varphi)$ is given by

$$\operatorname{supp} \mathfrak{D}\mathfrak{J}(\varphi) \subseteq \{V \in C^\infty(\mathbb{R}^{n+1}, \mathbb{R}^{n+1}) : \varphi(M) \cap \operatorname{supp} V \neq \varnothing\}. \tag{19}$$

(ii) There exist continuous linear functionals $g^{\mathcal{T}} : C^\infty(\mathbb{R}^{n+1}, \mathbb{R}^{n+1}) \to \mathbb{R}$ and $g^{\mathcal{N}} : C^\infty(\mathbb{R}^{n+1}, \mathbb{R}^{n+1}) \to \mathbb{R}$, depending on φ, which are tempered distributions when restricted to $C_c^\infty(\mathbb{R}^{n+1}, \mathbb{R}^{n+1})$ (see Rudin, 1991, Chapter 6.1, for definitions), with support on $\varphi(M)$ such that

$$\mathfrak{D}\mathfrak{J}(\varphi)[V] = \left\langle g^{\mathcal{N}}, V \right\rangle + \left\langle g^{\mathcal{T}}, V \right\rangle \qquad \forall V \in C^\infty(\mathbb{R}^{n+1}, \mathbb{R}^{n+1}) \tag{20}$$

with

$$\operatorname{supp} g^{\mathcal{N}} \subseteq \operatorname{supp} \mathfrak{D}\mathfrak{J}(\varphi) \cap \{V \in C_c^\infty(\mathbb{R}^{n+1}, \mathbb{R}^{n+1}) : \mathrm{Tr}_{|\varphi(M)}[V] \in \mathcal{N}_{\varphi(M)}\} \tag{21}$$

and

$$\operatorname{supp} g^{\mathcal{T}} \subseteq \operatorname{supp} \mathfrak{D}\mathfrak{J}(\varphi) \cap \{V \in C_c^\infty(\mathbb{R}^{n+1}, \mathbb{R}^{n+1}) : \mathrm{Tr}_{|\varphi(M)}[V] \in \mathcal{T}_{\varphi(M)}\}, \tag{22}$$

where $\mathrm{Tr}_{|\varphi(M)} : C^\infty(\mathbb{R}^{n+1}, \mathbb{R}^{n+1}) \to C^\infty(\varphi(M), \mathbb{R}^{n+1})$ is the trace operator and n the outer unit normal vector field on $\varphi(M)$.

(iii) If $\mathfrak{J}$ has shape functionality, then for all $\varphi \in \mathrm{Emb}(M, \mathbb{R}^{n+1})$, we have $g^{\mathcal{T}} = 0$ and

$$\mathfrak{D}\mathfrak{J}(\varphi)[V] = \mathcal{D}\mathcal{J}(\pi(\varphi))[V] \qquad \forall V \in C^\infty(\mathbb{R}^{n+1}, \mathbb{R}^{n+1}), \tag{23}$$

where $\mathcal{J} : B_e^n \to \mathbb{R}$ is the natural shape functional corresponding to $\mathfrak{J}$ by $\mathcal{J} \circ \pi = \mathfrak{J}$. In particular, $g^{\mathcal{N}}$ corresponds to the distribution of the classical Hadamard-Zolésio structure theorem.

Proof Since we are in a different situation than that of the classical Hadamard-Zolésio structure theorem, see Delfour and Zolésio (2001, Chapter 9, Theorem 3.6) for (i) and (ii), we give proofs for these ourselves.

For (i), let $V \in C^\infty(\mathbb{R}^{n+1}, \mathbb{R}^{n+1})$ be such that $\varphi(M) \cap \operatorname{supp} V = \varnothing$. Consider the perturbation of identity φ_t for V of φ as in eq. (12). By $\varphi(M) \cap \operatorname{supp} V = \varnothing$ we have $V \circ \varphi = 0$, resulting in $\varphi_t = \varphi$ being constant in t. This yields $\mathfrak{D}\mathfrak{J}(\varphi)[V] = 0$ by eq. (13), which immediately gives us (i).

For (ii), the proof, to some extent, follows analogous reasoning as in Delfour and Zolésio (2001, Chapter 9.3.4, Corollary 1), where Banach spaces $C^k(\mathbb{R}^{n+1}, \mathbb{R}^{n+1})$ are considered. It is clear that $\mathfrak{D}\mathfrak{J}(\varphi) : C^\infty(\mathbb{R}^{n+1}, \mathbb{R}^{n+1}) \to \mathbb{R}$ defines a linear functional with compact support as in eq. (19) (see Rudin, 1991, Definition 6.22, for definition of supports of distributions). In addition, we can use the fact that it is contained in the Schwartz space $C_c^\infty(\mathbb{R}^{n+1}, \mathbb{R}^{n+1})$, due to compactness of $\varphi(M)$. This gives us the tempered distribution property. Then, $g^{\mathcal{T}}$ and $g^{\mathcal{N}}$ are defined by restriction to the vertical and horizontal parts of V, recurring on decomposition of the tangent bundle in horizontal and vertical components of 5, giving us (ii).

For (iii), let $\mathfrak{J}$ have shape functionality and let $V \in C^\infty(\mathbb{R}^{n+1}, \mathbb{R}^{n+1})$. On $\varphi(M)$, we can decompose V into normal and tangential components. For the tangential part, we can follow analogous arguments as in the proof of Proposition 1, giving us a curve φ_t in the fiber $\pi(\varphi)$, generating the pre-shape derivative as a differential at a given φ. As φ_t is running on the fiber of φ and $\mathfrak{J}$ has shape functionality (see Definition 2) in φ by assumption, $\mathfrak{J}(\varphi_t)$ is constant for all t, rendering $g^{\mathcal{T}} = 0$ by eq. (20). Further, by eq. (20), the pre-shape derivative $\mathfrak{D}\mathfrak{J}(\varphi)[V]$ reduces to $g^{\mathcal{N}}$ acting on normal directions. With Proposition 1, shape functionality of $\mathfrak{J}$ leads to a well defined shape functional $\mathcal{J} : B_e^n \to \mathbb{R}$ with $\mathcal{J} \circ \pi = \mathfrak{J}$. As the tangential part of V has no impact on $\mathfrak{D}\mathfrak{J}(\varphi)[V]$, we can find a horizontal curve φ_t generating $\mathfrak{D}\mathfrak{J}(\varphi)[V]$. The representative φ_t either creates a trivial curve $\pi(\varphi_t)$ in B_e^n, which leads to eq. (23) being 0 on both sides, or a non-trivial curve $\pi(\varphi_t)$ in B_e^n. If $\pi(\varphi_t)$ is non trivial, we have

$$\mathcal{D}\mathcal{J}(\pi(\varphi))[V] = \frac{\mathrm{d}}{\mathrm{d}t}_{|t=0} \mathcal{J}(\pi(\varphi_t)) = \frac{\mathrm{d}}{\mathrm{d}t}_{|t=0} \mathfrak{J}(\varphi_t) = \mathfrak{D}\mathfrak{J}(\varphi)[V] \tag{24}$$

for the shape derivative $\mathcal{D}\mathcal{J}(\pi(\varphi))$ and pre-shape derivative $\mathfrak{D}\mathfrak{J}(\varphi)$, resulting in eq. (23). By association of $\varphi(M)$ with $\pi(\varphi) \in B_e^n$ this also shows that $g^{\mathcal{N}}$ corresponds to the distribution in the classical Hadamard-Zolésio structure Theorem (see Delfour and Zolésio, 2001, Chapter 9.3.4, Theorem 3.6 and Corollary 1), giving us (iii). □

The structure Theorem 1 gives an intuitive way to understand the pre-shape derivative, eq. (13), and the relation between shape functionals and pre-shape functionals. Part (i) of Theorem 1 has the same meaning as in the classical Hadamard-Zolésio structure theorem for shape derivatives, namely that deformations of the hold-all domain only influence the pre-shape functional if they deform the (pre-) shape $\varphi(M)$.

The difference with respect to classical shape derivatives is illustrated in equation (20), where the effect of deformations on the objective is split into normal and tangential components. The normal part $g^{\mathcal{N}}$ can be understood as the shape optimization part of $\mathfrak{D}\mathfrak{J}$, i.e. $\mathfrak{J}$ depending on the change of interface $\varphi(M)$. This is also reflected by the structure of its support, given in eq. (21), which states that only normal directions $V \in \mathcal{N}_{\varphi(M)}$, deforming $\varphi(M)$, have an effect on $g^{\mathcal{N}}$. On the other hand, $g^{\mathcal{T}}$ is interpretable as the part of $\mathfrak{D}\mathfrak{J}$ being sensitive to reparameterization of the shape $\varphi(M)$, which is shown by the structure of its support in eq. (22), where only tangential vector field $V \in \mathcal{T}_{\varphi(M)}$ plays a role. In classical shape optimization, tangential vectors are always in the nullspace of the shape derivative. But in the more general pre-shape case both components discussed can have non-trivial effects.

This is also reflected by Theorem 1 (*iii*), stating that pre-shape functionals having shape functionality have vanishing tangential part of the pre-shape derivative $\mathfrak{D}\mathfrak{J}$, meaning that they are only supported by normal components of the deformation field $V \in C^\infty(\mathbb{R}^{n+1}, \mathbb{R}^{n+1})$ just as in the classical shape optimization theory. On the other hand, if 'shape derivatives' are not found to vanish in tangential directions, the 'shape functional' at hand is actually a true pre-shape functional. This is the case for mesh optimization techniques we will introduce.

Also, for shapes $\varphi(M) \subset \mathbb{R}^{n+1}$ being bounded and topologically closed C^{k+1}-submanifolds of $\mathbb{R}^{n+1}$ with non-empty interior, the classical Hadamard-Zolésio structure theorem was generalized in Sturm (2016, Theorem 5.5). In the special case of the objective $\mathfrak{J}$ having shape functionality, i.e. vanishing tangential component of the pre-shape derivative as by Theorem 1, the results of Sturm (2016, Corollary 4.2) coincide with results in Theorem 1.

Before we come to some exemplary pre-shape derivatives and their decompositions, we formulate a simple corollary, which connects the classical material derivatives with their pre-shape versions.

Corollary 1 (Decomposition for Pre-Shape Material Derivatives) *Let* $f : \mathrm{Emb}(M, \mathbb{R}^{n+1}) \times \mathbb{R}^{n+1} \to \mathbb{R}$ *be pre-shape differentiable,* $\varphi \in \mathrm{Emb}(M, \mathbb{R}^{n+1})$ *and* $V \in C^\infty(\mathbb{R}^{n+1}, \mathbb{R}^{n+1})$.
Then, the material derivative decomposes into

$$\mathfrak{D}_m f(\varphi)[V] = \left\langle g^{\mathcal{N}}, V \right\rangle + \left\langle g^{\mathcal{T}}, V \right\rangle + \nabla f_\varphi^T V. \tag{25}$$

In particular, if f *has shape functionality, then for the corresponding shape dependent function* $\tilde{f} : B_e \times \mathbb{R}^{n+1} \to \mathbb{R}$ *the relationship*

$$\mathfrak{D}_m f(\varphi)[V] = \mathcal{D}_m \tilde{f}(\pi(\varphi))[V] \tag{26}$$

holds for all $\varphi \in \mathrm{Emb}(M, \mathbb{R}^{n+1})$*, which means that the pre-shape and classical material derivative coincide.*

Proof To get the decomposition of eq. (25), we simply use the formula of eq. (18) and apply decomposition, eq. (20), of the structure theorem to the

occurring pre-shape derivatives for fixed $x_0 \in \mathbb{R}^{n+1}$. If f has shape functionality, we can apply part (*iii*) of Theorem 1 to decomposition of eq. (25) and see that the pre-shape material derivative equals the classical material derivative $\mathcal{D}_m \tilde{f}(\pi(\varphi))[V]$, since $g^{\mathcal{N}}$ corresponds to the distribution from the classical Hadamard theorem. □

With the last part of this corollary, we can apply the pre-shape material derivatives to shape differentiable functions, yielding the same results as the classical material derivative by association with pre-shape extensions via Proposition 1.

We have now seen that Structure Theorem 1, Proposition 1 and Corollary 1 guarantee validity of the classical shape calculus formulae and results in the context of pre-shapes. Pre-shape calculus can be applied to objects from shape optimization if they are associated with their corresponding pre-shape counterparts, leading to the same derivatives and thus optimization methods. Even further, it is possible to apply pre-shape calculus to mixed shape and pre-shape problems, where the shape part is treated just as if shape calculus were applied, with the key difference being that a pre-shape component would otherwise be non-accessible. In the following, we show some simple examples, which are not accessible by classical shape calculus.

EXAMPLE 1 For a target pre-shape $\tilde{\varphi} \in \mathrm{Emb}(S^1, \mathbb{R}^2)$, let us define a pre-shape optimization problem by

$$\min_{\varphi \in \mathrm{Emb}(S^1,\mathbb{R}^2)} \frac{1}{2} \int_{S^1} |\varphi - \tilde{\varphi}|^2 \, \mathrm{d}s \; =: \mathfrak{J}(\varphi). \tag{27}$$

The pre-shape functional $\mathfrak{J}$ measures the difference of a target $\tilde{\varphi}$ to another parameterized shape φ.

Its pre-shape derivative can be calculated for directions $V \in C^\infty(\mathbb{R}^2, \mathbb{R}^2)$ by using elementary techniques

$$\begin{aligned} \mathfrak{D}\mathfrak{J}(\varphi)[V] =& \frac{\mathrm{d}}{\mathrm{d}t}_{|t=0} \frac{1}{2} \int_{S^1} |\varphi_t - \tilde{\varphi}|^2 \, \mathrm{d}s \\ =& \frac{1}{2} \int_{S^1} \frac{\mathrm{d}}{\mathrm{d}t}_{|t=0} \langle \varphi + t \cdot V \circ \varphi - \tilde{\varphi}, \varphi + t \cdot V \circ \varphi - \tilde{\varphi} \rangle \, \mathrm{d}s \\ =& \int_{S^1} \langle \varphi - \tilde{\varphi}, V \circ \varphi \rangle \, \mathrm{d}s. \end{aligned} \tag{28}$$

We can choose S^1 with canonical parameterization as a starting pre-shape or point of reference by considering

$$\varphi_{id} : S^1 \subset \mathbb{R}^2 \to \mathbb{R}^2, \begin{pmatrix} x_1 \\ x_2 \end{pmatrix} \mapsto \begin{pmatrix} x_1 \\ x_2 \end{pmatrix}. \tag{29}$$

In order to formulate the Hadamard-Zolésio-type decomposition, eq. (20), we need the outer normal vector field and an oriented tangential vector field, which

for S^1 are given by

$$n : S^1 \to \mathbb{R}^2, \begin{pmatrix} x_1 \\ x_2 \end{pmatrix} \mapsto \begin{pmatrix} x_1 \\ x_2 \end{pmatrix}, \quad \tau : S^1 \to \mathbb{R}^2, \begin{pmatrix} x_1 \\ x_2 \end{pmatrix} \mapsto \begin{pmatrix} -x_2 \\ x_1 \end{pmatrix}. \tag{30}$$

Now, we can examine the problem for several different parameterized target shapes $\tilde{\varphi} \in \mathrm{Emb}(S^1, \mathbb{R}^2)$. First, we can consider rescaling by a factor $\alpha \in (0, \infty)$, which lets S^1 contract or expand. The target for this is given by

$$\tilde{\varphi} : S^1 \to \mathbb{R}^2, \begin{pmatrix} x_1 \\ x_2 \end{pmatrix} \mapsto \alpha \cdot \begin{pmatrix} x_1 \\ x_2 \end{pmatrix}. \tag{31}$$

Using eq. (28), the pre-shape derivative becomes

$$\mathfrak{D}\mathfrak{J}(\varphi_{id})[V] = \int_{S^1} (1 - \alpha) \cdot \langle n, V \rangle \, \mathrm{d}s. \tag{32}$$

This shows that rescaling of S^1 has vanishing parameterization part $g^{\mathcal{T}} \equiv 0$, whereas the remaining shape component $g^{\mathcal{N}}$ is in the style of the classical Hadamard-Zolésio representation, given above. In particular, only vector fields V acting in normal direction are supported.

Next, let us consider a rotation of the circle. For this, we let $\alpha \in [0, 2\pi)$ and consider target rotations

$$\tilde{\varphi} : S^1 \to \mathbb{R}^2, \begin{pmatrix} x_1 \\ x_2 \end{pmatrix} \mapsto \begin{pmatrix} \cos(\alpha) & -\sin(\alpha) \\ \sin(\alpha) & \cos(\alpha) \end{pmatrix} \begin{pmatrix} x_1 \\ x_2 \end{pmatrix}. \tag{33}$$

Plugging this into eq. (28) and doing some reformulations, the according decomposition becomes

$$\mathfrak{D}\mathfrak{J}(\varphi_{id})[V] = \int_{S^1} \big(1 - \cos(\alpha)\big) \cdot \langle n, V \rangle \, \mathrm{d}s + \int_{S^1} \sin(\alpha) \cdot \langle \tau, V \rangle \, \mathrm{d}s. \tag{34}$$

Here we see both components of the decomposition, the first corresponding to the normal $g^{\mathcal{N}}$, and the second corresponding to the tangential part $g^{\mathcal{T}}$. Notice that the normal component vanishes exactly for trivial rotations, whereas the tangential part also vanishes for the reflection at origin case, $\alpha = \pi$.

Finally, we can also translate S^1 by some fixed $z \in \mathbb{R}^2$, which gives a target

$$\tilde{\varphi} : S^1 \to \mathbb{R}^2, \begin{pmatrix} x_1 \\ x_2 \end{pmatrix} \mapsto \begin{pmatrix} x_1 \\ x_2 \end{pmatrix} + z. \tag{35}$$

The decomposition of the pre-shape derivative becomes

$$\mathfrak{D}\mathfrak{J}(\varphi_{id})[V] = \int_{S^1} \langle n, z \rangle \cdot \langle n, V \rangle \, \mathrm{d}s + \int_{S^1} \langle \tau, z \rangle \cdot \langle \tau, V \rangle \, \mathrm{d}s, \tag{36}$$

where decomposition into $g^{\mathcal{N}}$ and $g^{\mathcal{T}}$ depends on normal and tangential components of z on S^1.

Next, we give a summary of several useful pre-shape calculus formulae. Due to Proposition 1 and Corollary 1, they are also true for shape derivatives and functionals.

Corollary 2 (Pre-Shape Calculus Rules) *Let f, g: $\mathrm{Emb}(M, \mathbb{R}^{n+1}) \times \mathbb{R}^{n+1} \to \mathbb{R}$ be pre-shape differentiable and differentiable in the second component, and let $h : \mathbb{R} \to \mathbb{R}$ be differentiable. Let $\Omega \subseteq \mathbb{R}^{n+1}$ be an open, bounded domain with Lipschitz boundary, Γ an n-dimensional C^∞-submanifold of $\mathbb{R}^{n+1}$. Consider $\varphi \in \mathrm{Emb}(M, \mathbb{R}^{n+1})$ and $V \in C^\infty(\mathbb{R}^{n+1}, \mathbb{R}^{n+1})$. Then, the following set of rules applies for pre-shape and -material derivatives, including the special case of shape derivatives.*

$$
\begin{aligned}
&(i)\ \mathfrak{D}_m f(\varphi)[V] && = \mathfrak{D} f(\varphi)[V] + \nabla f_\varphi^T V \\
&(ii)\ \mathfrak{D}_m (f \cdot g)(\varphi)[V] && = \mathfrak{D}_m f(\varphi)[V] \cdot g_\varphi + f_\varphi \cdot \mathfrak{D}_m g(\varphi)[V] \\
&(iii)\ \mathfrak{D}_m (h \circ f)(\varphi)[V] && = Dh(f_\varphi) \mathfrak{D}_m f(\varphi)[V] \\
&(iv)\ \mathfrak{D}\left(\textstyle\int_\Omega f \,\mathrm{d}x\right)(\varphi)[V] && = \textstyle\int_\Omega \mathfrak{D}_m f(\varphi)[V] + \mathrm{div}(V) f_\varphi \,\mathrm{d}x \\
&(v)\ \mathfrak{D}\left(\textstyle\int_\Gamma f \,\mathrm{d}s\right)(\varphi)[V] && = \textstyle\int_\Gamma \mathfrak{D}_m f(\varphi)[V] + \mathrm{div}_\Gamma(V) f_\varphi \,\mathrm{d}s
\end{aligned}
$$

with $\mathrm{div}_\Gamma(V)$ being the tangential divergence of V on φ, and Dh being the total derivative of h.

Proof Let the assumptions stated above hold. Identity (i) was already discussed in Corollary 1.

The product- and chain-rule (ii) and (iii) are simple consequences of the definition of the material derivative eq. (17).

For (iv), the conditions for Henrot and Pierre (2018, Theorem 5.2.2) apply by considering $f_{\varphi_t}(x_t)$, a function of $t \geq 0$. Alternatively, since we assumed Lipschitz boundary for Ω, the change of variable formula is applicable and the standard proof, found in Haslinger and Mäkinen (2003, p. 112, Lemma 3.3) can be used as well.

The situation for (v) is more involved. For this, we refer the reader to Henrot and Pierre (2018, Theorem 5.4.17) or Delfour and Zólesio (2001, Chapter 9.4, Theorem 4.3). □

Remark 2 (Weakening Assumptions for Pre-Shape Calculus) *The formulae provided in Corollary 2 hold in far greater generality.*

In particular, the chain rule (iii) can be stated for Fréchet differentiable operators h on Banach spaces of continuous functions with the help of Delfour and Zólesio (2001, Chapter 9, Theorem 2.5).

Also, formula (iv) for volume integrals can be stated for domains Ω which are merely measurable, and pre-shape differentiable families of class

$$\{f_\varphi \in W^{1,1}(\mathbb{R}^{n+1}, \mathbb{R})\}_{\varphi \in \mathrm{Emb}(M, \mathbb{R}^{n+1})}$$

with the use of Henrot and Pierre (2018, Theorem 5.2.2).

Finally, formula (v) for boundary integrals can be generalized to compact hypersurfaces $\Gamma \subset \mathbb{R}^{n+1}$ of C^1-regularity and pre-shape differentiable families

of class $\{f_\varphi \in W^{1,1}(\mathbb{R}^{n+1}, \mathbb{R})\}_{\varphi \in \mathrm{Emb}(M,\mathbb{R}^{n+1})}$ *by the use of Henrot and Pierre (2018, Theorem 5.4.17).*

Example 2 (Pre-Shape Parameterization Tracking Problem) With this problem class we introduce a non-trivial example for pre-shape optimization problems. Its pre-shape derivative, in fact, is not a classical shape derivative, and thus is not tractable by shape calculus. Later on, this problem class will enable us to optimize the overall mesh quality of discretizations and representations of shapes similar to deformation methods going back to Liao and Andersen (1992). To be specific, the fiber bundle structure of $\mathrm{Emb}(M, \mathbb{R}^{n+1})$ offers the possibility to modify a given shape optimization problem in such a way, that the original solution is maintained, while at the same time optimization for the parameterization can take place. This gives rise to several different mesh regularization algorithms, and justifies the numerical optimization procedures we will establish in future works.

Before we further elaborate on this, we introduce the necessary vocabulary and notation to formulate our problem in $\mathrm{Emb}(M, \mathbb{R}^{n+1})$ for submanifolds $M \subset \mathbb{R}^{n+1}$. First, we need the concept of *local frames*, which are the local orthonormal bases of tangential vectors on M (see Lee, 2013, Chapter 8). For an open subset $U \subseteq M$, a smooth local frame is a tuple of $\dim(M)$ tangential vector fields $\tau := (\tau_1, \dots, \tau_n)$, such that for each $p \in U$ the tangential vectors $\tau_i(p) \in T_pM$ are linearly independent. If we have a Riemannian metric on M, then we can additionally demand $\tau(p) = (\tau_1(p), \dots, \tau_n(p))$ to be orthonormal with respect to the Riemannian metric for all $p \in U$, thus calling the frame $(\tau_1, \dots, \tau_n)$ *local orthonormal frame*. Note that local orthonormal frames always exist, due to the simple use of the Gram-Schmidt algorithm in tangential spaces (see Lee, 2013, Lemma 8.13).

To achieve a natural and numerically tractable formulation of a pre-shape parameterization tracking problem, we also need to introduce the covariant derivative of an embedding $\varphi \in \mathrm{Emb}(M, \mathbb{R}^{n+1})$. For this, we use similar ideas as in Delfour and Zólesio (2001, Chapter 9.5.6) and modify them to our situation using local orthonormal frames. Given a $\varphi \in \mathrm{Emb}(M, \mathbb{R}^{n+1})$, let $\tau : U \to (TM)^n$ be a smooth local orthonormal frame on $U \subseteq M$ and let $\tau^\varphi : V \to (T\varphi(M))^n$ be a local orthonormal frame on $V \subseteq \varphi(M)$. Without loss of generality, we can assume $V = \varphi(U)$, since we can choose $V = V \cap \varphi(U)$. Then, we define the local *covariant derivative* representation for φ under the choice of frames τ and τ^φ by

$$D^\tau \varphi_{|U}(p) := \begin{pmatrix} \langle D\varphi\tau_{1,p}, \tau^\varphi_{1,\varphi(p)} \rangle & \dots & \langle D\varphi\tau_{n,p}, \tau^\varphi_{1,\varphi(p)} \rangle \\ \vdots & \ddots & \vdots \\ \langle D\varphi\tau_{1,p}, \tau^\varphi_{n,\varphi(p)} \rangle & \dots & \langle D\varphi\tau_{n,p}, \tau^\varphi_{n,\varphi(p)} \rangle \end{pmatrix}, \tag{37}$$

where $D\varphi$ is the Jacobian matrix of φ and $\langle ., . \rangle$ the Euclidean scalar product of $\mathbb{R}^{n+1}$. We want to make clear that the covariant derivative $D^\tau \varphi$ should not be

mistaken for the tangential derivative $D_\Gamma\varphi$, which is given by (see Delfour and Zólesio, 2001, Chapter 9.5.2)

$$D_\Gamma\varphi = D\varphi - D\varphi nn^T. \tag{38}$$

Having numerical implementations in mind, we are also interested in the case of shapes with non-trivial boundaries. However, when the boundary is non-trivial, we impose restrictions on the pre-shapes permitted. Specifically, embeddings leaving the boundary invariant are sufficient, i.e.

$$\mathrm{Emb}_{\partial M}(M, \mathbb{R}^{n+1}) := \{\varphi \in \mathrm{Emb}(M, \mathbb{R}^{n+1}) : \varphi(p) = p \quad \forall p \in \partial M\}. \tag{39}$$

For numerical routines this means that a specified boundary ∂M of the starting shape is left fixed, whereas the interior of the shape is able to deform and change its shape and parameterization. In the case of empty boundary, the pre-shape space becomes $\mathrm{Emb}(M, \mathbb{R}^{n+1})$, meaning that shapes are allowed to move freely.

With the introduction of covariant derivatives and appropriate pre-shapes for the boundary case, we can formulate a *pre-shape parameterization tracking problem*, inspired by a least-squares formulation of the deformation method for mesh element volume optimization, as found in Cai, Jiang and Liao (2004), Cao, Huang and Russell (2002) and Grajewski, Köster and Turek (2009). We remind the reader that mesh deformation methods search for a specified target cell volume f by changing coordinates of nodes. For our formulation, we take a slight twist by using inverse Jacobians, which changes the interpretation of optimal φ and targets f_φ. In our case, f_φ describes the desired local density of mesh nodes, whereas the authors of Cai, Jiang and Liao (2004), Cao, Huang and Russell (2002), and Grajewski, Köster and Turek (2009) use targets f, describing the local cell volume. For this reason, the authors mentioned need to use reciprocals of f, instead of reciprocals of Jacobians. Still, both formulations are equivalent by inverting the solutions, Jacobians and targets. In addition to targets f_φ, we also incorporate a positive function $g^M : M \to (0, \infty)$, which will act as the distribution of nodes for the initial mesh.

The following proposition gives the definition, well-definedness and existence of solutions of the pre-shape parameterization tracking problem.

Proposition 2 (Pre-Shape Parameterization Tracking Problem and Existence of Solutions) *Let M be an n-dimensional, orientable, path-connected and compact C^∞-submanifold of $\mathbb{R}^{n+1}$, possibly with non-empty boundary ∂M of C^∞-regularity. Additionally, let $g^M : M \to (0, \infty)$ and $f_\varphi : \varphi(M) \to (0, \infty)$ be C^∞-functions, with f having shape functionality. Further, assume the normalization condition*

$$\int_{\varphi(M)} f_\varphi(s)\, \mathrm{d}s = \int_M g^M(s)\, \mathrm{d}s \quad \forall \varphi \in \mathrm{Emb}_{\partial M}(M, \mathbb{R}^{n+1}). \tag{40}$$

Then the following problem

$$\min_{\varphi\in \mathrm{Emb}_{\partial M}(M,\mathbb{R}^{n+1})} \frac{1}{2}\int_{\varphi(M)} \left(g^M\circ\varphi^{-1}(s)\cdot\frac{1}{\det D^\tau\varphi\circ\varphi^{-1}(s)} - f_\varphi(s)\right)^2 \mathrm{d}s \quad (41)$$

is called pre-shape parameterization tracking problem. *It is well-defined and independent of choice of local orthornormal frames τ, τ_φ on M and $\varphi(M)$. Further, in each fiber $\pi(\varphi)$ there exists a global C^∞-solution to the problem of eq.* (41)*, i.e. an embedding $\tilde{\varphi}$, satisfying*

$$(g^M\circ\tilde{\varphi}^{-1})\cdot\det D^\tau\tilde{\varphi}^{-1} \equiv f_\varphi \quad \textit{and} \quad \tilde{\varphi}(p) = p \quad \forall p\in\partial\tilde{\varphi}(M). \quad (42)$$

Proof The main ingredient of this proof is a theorem by Moser (1965), extended by Dacorogna and Moser (1990) in their Theorem 1, which guarantees existence solutions. Due to the quadratic nature of the objective functional, it is obvious that eq. (42) is a sufficient condition for optimality. Together with normalization condition, eq. (40), Moser's and Dacorogna's theorem guarantees existence of embeddings satisfying eq. (42), which is a polynomial PDE, by application of Laplace's formula for determinants.

Fix an orientation for M, $\varphi\in\mathrm{Emb}_{\partial M}(M,\mathbb{R}^{n+1})$ and let τ, τ^φ be local orthonormal frames for each $\varphi\in\mathrm{Emb}_{\partial M}(M,\mathbb{R}^{n+1})$. Well-definedness of the integrand in the problem of eq. (41) is clear, since g^M is positive and φ is an immersion, making $D^\tau\varphi\in GL(n,\mathbb{R})$, and thus $\det D^\tau\varphi$ non-vanishing. In the case of non-empty boundary, the integral is well-defined by using the interior of $\varphi(M)$, as the boundary ∂M is a set of measure zero. Independence of choice of orientation preserving local orthonormal bases inducing the covariant derivative (see eq. (37)) is also clear, since an orientation preserving change of the orthonormal base can be realized by multiplications with orthogonal matrices $\tilde{B}, B\in SO(n)$, and hence, by the determinant product rule, $\det D^\tau\varphi$ remains invariant. Further, if no global orthonormal frame exists, well-definedness and independence of choice of local orthonormal frames is guaranteed as well. This can be ensured by using a partition of unity, which covers $\varphi(M)$ with open domains of local orthonormal frames, and linearity of the integral in eq. (41) together with the previous argument about the change of orthonormal bases. □

Remark 3 (Hölder Regularity Case) *The existence and well-definedness result from Proposition 2 also holds in the more general context of $C^{k,\alpha}$-Hölder re-gularity. For given $k\in\mathbb{N}$ and $\alpha\in(0,1)$, if M, f_φ and g^M have $C^{k,\alpha}$-regularity, and ∂M has $C^{k+3,\alpha}$ regularity, then solutions φ with $C^{k+1,\alpha}$-regularity exist in each fiber. This stems from the regularity results in Dacorogna and Moser (1990).*

Having guaranteed the existence of solutions, we want to turn our attention to the pre-shape derivative of the parameterization tracking problem, eq. (41). This serves several different purposes in our studies. First, it is of numerical interest, since we will construct several algorithms for improvement of mesh

quality in shape optimization routines based on derivatives. At the same time, eq. (41) serves as a non-trivial example to illustrate the application of pre-shape calculus techniques, developed in Section 2. In particular, we will see that the derivative to the general parameterization tracking problem, eq. (41), is not accessible via the classical shape calculus techniques. In the following, we will leave the target density functions f_φ general and only assume enough regularity for the existence of the pre-shape derivative. Later in this article, we will propose an explicit way to construct f_φ (see monitor function study by Cao, Huang and Russell, 1999), while also ensuring existence of its material derivatives with a closed form (cf. Section 2.5).

As we permit non-empty boundaries left to be invariant in the parameterization tracking problem, the space of possible test functions V is altered in an according way. In particular, due to invariance of ∂M, vector fields for $\mathrm{Emb}_{\partial M}(M, \mathbb{R}^{n+1})$ are given by vector fields vanishing on the boundary (see Ebin and Marsden, 1970, Theorem 8.2; Smolentsev, 2007, Theorem 3.19), i.e.

$$C^\infty_{\partial M}(\mathbb{R}^{n+1}, \mathbb{R}^{n+1}) := \{V \in C^\infty(\mathbb{R}^{n+1}, \mathbb{R}^{n+1}) : \mathrm{Tr}_{|\partial M}(V) = 0\}. \tag{43}$$

Of course, the same is true for Hölder and Sobolev regularities. With this in mind, we can derive the pre-shape derivative of the parameterization tracking problem.

Theorem 2 *(*Pre-Shape Derivative of the Pre-Shape Parameterization Tracking Problem*) Let the assumptions of Proposition 2 hold and denote by $\mathfrak{J}^\tau$ the objective functional of the general parameterization tracking problem of eq.* (41)*. Also, assume enough regularity for f_φ, such that material derivatives exist.*

Then, for fixed $\varphi \in \mathrm{Emb}_{\partial M}(M, \mathbb{R}^{n+1})$ and $V \in C^\infty_{\partial\varphi(M)}(\mathbb{R}^{n+1}, \mathbb{R}^{n+1})$, the pre-shape derivative of eq. (41) *is given by*

$$\begin{aligned}\mathfrak{D}\mathfrak{J}^\tau(\varphi)[V] = -\int_{\varphi(M)} \frac{1}{2} \cdot \Big(\big(g^M \circ \varphi^{-1} \cdot \frac{1}{\det D^\tau \varphi} \circ \varphi^{-1}\big)^2 - f_\varphi^2 \Big) \cdot \mathrm{div}_\Gamma(V) \\ + \Big(g^M \circ \varphi^{-1} \cdot \frac{1}{\det D^\tau \varphi} \circ \varphi^{-1} - f_\varphi \Big) \cdot \mathfrak{D}_m(f_\varphi)[V] \, \mathrm{d}s,\end{aligned} \tag{44}$$

with $\mathfrak{D}_m(f_\varphi)$ being the pre-shape material derivative of f_φ and div_Γ the tangential divergence on $\varphi(M)$. The pre-shape derivative does not depend on the choice of oriented local orthonormal frames τ, τ^φ for representing the covariant derivative D^τ.

Proof For the proof we rely on pre-shape calculus rules we have established in Section 2. In particular, we will make use of formulae found in Corollary 2. So, let M fulfill the assumptions made in Theorem 2. Fix a $\varphi \in \mathrm{Emb}_{\partial M}(M, \mathbb{R}^{n+1})$ and let $V \in C^\infty_{\partial\varphi(M)}(\mathbb{R}^{n+1}, \mathbb{R}^{n+1})$. The following arguments are all valid for $C^{k,\alpha}$-regularity.

The use of pre-shape material derivative makes sense for families of differentiable functions on varying domains $\{f_\varphi : \varphi(M) \to \mathbb{R}\}_{\varphi\in \mathrm{Emb}_{\partial M}(M,\mathbb{R}^{n+1})}$ depending smoothly on φ, since the limit $\mathfrak{D}_m f(\varphi)[V]$ involves the term $f_{\varphi_t}(x_t)$. An easy check reveals that the term is well defined, due to Definition 4 of moving points x_t and the perturbation of identity for pre-shapes, eq. (12), coinciding

$$x_t = x_0 + t\cdot V(x_0) = \varphi(\varphi^{-1}(x_0)) + t\cdot V\circ\varphi(\varphi^{-1}(x_0)) = \varphi_t(\varphi^{-1}(x_0)) \in \varphi_t(M). \tag{45}$$

However, note that in this case there is no decomposition of type of eq. (18) for $\mathfrak{D}_m f(\varphi)$, since $x_t \notin \varphi(M)$ and $x_0 \notin \varphi_t(M)$ in general.

With this in mind, we can apply Corollary 2 (v) to eq. (41) in order to get

$$\begin{aligned}\mathfrak{D}\mathfrak{J}^\tau(\varphi)[V] = \int_{\varphi(M)} &\mathfrak{D}_m\Big(\frac{1}{2}\big(g^M\circ\varphi^{-1}\cdot\frac{1}{\det D^\tau\varphi}\circ\varphi^{-1} - f_\varphi\big)^2\Big)[V]\\ &+\frac{1}{2}\,\mathrm{div}_\Gamma(V)\Big(g^M\circ\varphi^{-1}\cdot\frac{1}{\det D^\tau\varphi}\circ\varphi^{-1} - f_\varphi\Big)^2\,\mathrm{d}s.\end{aligned} \tag{46}$$

For simplification of the material derivative of the integrand, we employ our assumption on the existence of material derivatives for f_φ, together with the chain- and product rule for material derivatives (from Corollary 2), to see

$$\begin{aligned}&\mathfrak{D}_m\Big(\frac{1}{2}\big(g^M\circ\varphi^{-1}\cdot\frac{1}{\det D^\tau\varphi}\circ\varphi^{-1} - f_\varphi\big)^2\Big)[V]\\ &= \big(g^M\circ\varphi^{-1}\cdot\frac{1}{\det D^\tau\varphi}\circ\varphi^{-1} - f_\varphi\big)\cdot\Bigg(\mathfrak{D}_m(g^M\circ\varphi^{-1})[V]\cdot\frac{1}{\det D^\tau\varphi}\circ\varphi^{-1}\\ &-g^M\circ\varphi^{-1}\cdot\frac{1}{(\det D^\tau\varphi)^2}\circ\varphi^{-1}\cdot\mathfrak{D}_m(\det D^\tau\varphi\circ\varphi^{-1})[V] - \mathfrak{D}_m(f_\varphi)[V]\Bigg).\end{aligned} \tag{47}$$

In the following, we examine the remaining material derivatives in Section 2.2, except for $\mathfrak{D}_m(f_\varphi)[V]$, as we let f_φ remain general. To avoid confusion, we remind the reader that we are confronted with mappings h taking two arguments, one explicitly being a pre-shape, making them operators of the form

$$h.(\cdot) := h(\cdot,\cdot) :\ \mathrm{Emb}_{\partial M}(M,\mathbb{R}^{n+1})\times M\to\mathbb{R},\ (\varphi,p)\mapsto h_\varphi(p). \tag{48}$$

We will use the following relationship of embeddings and the domain perturbation of identity

$$\varphi_t(p) = (T_t\circ\varphi)(p)\quad \forall p\in M \Leftrightarrow (\varphi_t^{-1}\circ T_t)(q) = \varphi^{-1}(q)\quad \forall q\in\varphi(M), \tag{49}$$

where φ_t is the perturbation of identity for pre-shapes (cf. eq. (12)) for sufficiently small $t>0$. If material derivatives of h are assumed to exist, eq. (49)

leads to the following elementary, but interesting, identity

$$\mathfrak{D}_m\big(h_\varphi \circ \varphi^{-1}\big)[V] = \frac{\mathrm{d}}{\mathrm{d}t}_{|t=0} h(\varphi_t, \varphi_t^{-1} \circ T_t) =$$
$$\frac{\mathrm{d}}{\mathrm{d}t}_{|t=0} h(\varphi_t, \varphi^{-1}) = \mathfrak{D}(h_\varphi)[V] \circ \varphi^{-1}. \tag{50}$$

Applying this to the first remaining material derivative in Section 2.2, we get

$$\mathfrak{D}_m\big(g^M \circ \varphi^{-1}\big)[V] = \mathfrak{D}(g^M)[V] \circ \varphi^{-1} = 0, \tag{51}$$

since g^M is does not depend on the choice of $\varphi \in \mathrm{Emb}(M, \mathbb{R}^{n+1})$.

Next, we apply analogous techniques to the second material derivative. Hence, for calculation of the material derivative of $\det D^\tau\varphi \circ \varphi^{-1}$ it is sufficient to calculate its pre-shape derivative. Also, since the flow $(\varphi_t)_{t\in[0,\varepsilon)}$ given by the perturbation of identity in direction V (cf. eq. (12)) is differentiable in t, we can employ Jacobi's formula for the derivative of the determinant at $t_0 = 0$, to arrive at

$$\begin{aligned}\mathfrak{D}_m\big(\det D^\tau\varphi \circ \varphi^{-1}\big)[V] &= \Big(\frac{\mathrm{d}}{\mathrm{d}t}_{|t=t_0} \det D^\tau\varphi_t\Big) \circ \varphi^{-1} \\ &= \operatorname{tr}\Big(\operatorname{Adju}(D^\tau\varphi_{t_0})\frac{\mathrm{d}}{\mathrm{d}t}_{|t=t_0} D^\tau\varphi_t\Big) \circ \varphi^{-1} \\ &\overset{t_0=0}{=} \operatorname{tr}\Big(\operatorname{Adju}(D^\tau\varphi) D^\tau(V \circ \varphi)\Big) \circ \varphi^{-1},\end{aligned} \tag{52}$$

where $\operatorname{Adju}(\cdot)$ is the adjugate matrix and $\operatorname{tr}(\cdot)$ is the trace operator for matrices.

Knowing that $D^\tau\varphi$ is invertible for all $p \in M$ due to $\varphi \in \mathrm{Emb}(M, \mathbb{R}^{n+1})$, we can use Cramer's rule to express the adjugate in terms of inverses. Also, we can use invariance of the trace operator under permutations of multiplicative order of matrices, giving us

$$\begin{aligned}&\operatorname{tr}\Big(\operatorname{Adju}(D^\tau\varphi) D^\tau(V \circ \varphi)\Big) \circ \varphi^{-1} = \\ &= \operatorname{tr}\Big(\det(D^\tau\varphi) \cdot D^\tau\varphi^{-1} D^\tau(V \circ \varphi)\Big) \circ \varphi^{-1} \\ &= (\det D^\tau\varphi) \circ \varphi^{-1} \cdot \operatorname{tr}\Big((D^\tau\varphi)^{-1} D^\tau V(\varphi) D^\tau\varphi\Big) \circ \varphi^{-1} \\ &= (\det D^\tau\varphi) \circ \varphi^{-1} \cdot \operatorname{tr}\Big(D^\tau V(\varphi)\Big) \circ \varphi^{-1} \\ &= (\det D^\tau\varphi) \circ \varphi^{-1} \cdot \operatorname{div}_\Gamma(V).\end{aligned} \tag{53}$$

Using eq. (51) and eq. (53) in eq. (47), and plugging the material derivative into eq. (46), we arrive at

$$
\begin{aligned}
&\mathfrak{D}\mathfrak{J}^{\tau}(\varphi)[V] = \\
&\int_{\varphi(M)} \Big(g^M \circ \varphi^{-1} \cdot \frac{1}{\det D^{\tau}\varphi} \circ \varphi^{-1} - f_{\varphi}\Big) \\
&\qquad \cdot \Big(- g^M \circ \varphi^{-1} \cdot \frac{1}{\det D^{\tau}\varphi} \circ \varphi^{-1} \cdot \operatorname{div}_{\Gamma}(V) - \mathfrak{D}_m(f_{\varphi})[V]\Big) \\
&+ \frac{1}{2} \operatorname{div}_{\Gamma}(V) \Big(g^M \circ \varphi^{-1} \cdot \frac{1}{\det D^{\tau}\varphi} \circ \varphi^{-1} - f_{\varphi}\Big)^2 \, \mathrm{d}s \\
&= - \int_{\varphi(M)} \Big(g^M \circ \varphi^{-1} \cdot \frac{1}{\det D^{\tau}\varphi} \circ \varphi^{-1} - f_{\varphi}\Big) \\
&\qquad \cdot \left(\frac{1}{2} \Big(g^M \circ \varphi^{-1} \cdot \frac{1}{\det D^{\tau}\varphi} \circ \varphi^{-1} + f_{\varphi}\Big) \cdot \operatorname{div}_{\Gamma}(V) + \mathfrak{D}_m(f_{\varphi})[V] \right) \mathrm{d}s \\
&= - \int_{\varphi(M)} \frac{1}{2} \cdot \Big((g^M \circ \varphi^{-1} \cdot \frac{1}{\det D^{\tau}\varphi} \circ \varphi^{-1})^2 - f_{\varphi}^2 \Big) \cdot \operatorname{div}_{\Gamma}(V) \\
&\qquad\qquad + \Big(g^M \circ \varphi^{-1} \cdot \frac{1}{\det D^{\tau}\varphi} \circ \varphi^{-1} - f_{\varphi}\Big) \cdot \mathfrak{D}_m(f_{\varphi})[V] \, \mathrm{d}s, \qquad (54)
\end{aligned}
$$

which is the desired pre-shape derivative, eq. (44). The covariant derivative $D^{\tau}\varphi$, and hence also the pre-shape derivative, eq. (44), is independent of the choice of orthonormal frames by similar reasoning as in the first part of the proof of Proposition 2. □

In general cases, $\mathfrak{D}\mathfrak{J}^{\tau}(\varphi)[V]$ is non-vanishing for vector fields V tangential to $\varphi(M)$. By the structure theorem for pre-shape derivatives, Theorem 1, the globally vanishing tangential pre-shape derivatives indicate a functional, which is almost of classical shape functional type. If we take the form of the pre-shape derivative, as given in eq. (44), this clearly means that eq. (41) cannot be formulated as a shape optimization problem, nor is it tractable by classical shape calculus.

In the light of the main Structure Theorem 1 for pre-shape derivatives, we can further refine the representation of the pre-shape derivative, eq. (44), by decomposing it into normal and tangential parts. Interestingly, if the user wants to optimize for mesh quality by using pre-shape derivative based parameterization tracking, it is not recommendable to use the full pre-shape derivative, found in eq. (44). Instead, by decomposing the pre-shape derivative, we will see that the tangential component is sufficient for this task. If a special case of the pre-shape derivatives normal component is used, we recover numerical methods solving Plateau's problem by constructing minimal surfaces (see Dziuk, 1990; Pinkall and Polthier, 1993; Dziuk and Hutchinson, 1999). In some sense orthogonal to this, the use of tangential components gives algorithms resembling the deformation method for the optimization of mesh quality (see Liao and

Anderson, 1992; Grajewski, Köster and Turek, 2009; Cao, Huang and Russell, 1999).

2.3. Decomposing the pre-shape derivative

To derive this decomposition, notice the following informal relationship between tangential divergence and the mean curvature κ for hypersurfaces for $V \in C^\infty(\mathbb{R}^{n+1}, \mathbb{R}^{n+1})$ (see Lee, 2009, Definition 4.23)

$$\operatorname{div}_\Gamma(\langle V, n\rangle \cdot n) = (\nabla_\Gamma \langle V, n\rangle)^T n + \langle V, n\rangle \cdot \operatorname{div}_\Gamma(n) = \dim(M) \cdot \langle V, n\rangle \cdot \kappa, \quad (55)$$

due to orthogonality of tangential gradients $\nabla_\Gamma(\langle V, n\rangle)$ and the outer normal vector field n on the interior of $\varphi(M)$. Also, let us briefly assume $f_\varphi : \mathbb{R}^{n+1} \to \mathbb{R}$ mapping from the whole ambient space, which simplifies using normal derivatives of f_φ for the decomposition. With this, and the assumption of constant target parameterizations for each fiber, i.e. $f_\varphi = f_{\varphi\circ\rho}$ for all $\rho \in \operatorname{Diff}(M)$, we can refine eq. (44) to

$$\mathfrak{D}\mathfrak{J}^\tau(\varphi)[V] = \langle g_\varphi^{\mathcal{N}}, V\rangle + \langle g_\varphi^{\mathcal{T}}, V\rangle \quad \forall V \in C^\infty(\mathbb{R}^{n+1}, \mathbb{R}^{n+1}), \quad (56)$$

with shape (i.e. normal) component

$$\begin{aligned}\langle g_\varphi^{\mathcal{N}}, V\rangle = -\int_{\varphi(M)} \frac{\dim(M)}{2} \cdot \Big(\big(g^M \circ \varphi^{-1} \cdot \det D^\tau \varphi^{-1}\big)^2 - f_\varphi^2\Big) \cdot \kappa \cdot \langle V, n\rangle \\ + \Big(g^M \circ \varphi^{-1} \cdot \det D^\tau \varphi^{-1} - f_\varphi\Big) \cdot \Big(\frac{\partial f_\varphi}{\partial n} \cdot \langle V, n\rangle + \mathcal{D}(f_\varphi)[V]\Big)\, \mathrm{d}s \quad (57)\end{aligned}$$

and pre-shape (i.e. tangential) component

$$\begin{aligned}\langle g_\varphi^{\mathcal{T}}, V\rangle = -\int_{\varphi(M)} \frac{1}{2} \cdot \Big(\big(g^M \circ \varphi^{-1} \cdot \det D^\tau \varphi^{-1}\big)^2 - f_\varphi^2\Big) \cdot \operatorname{div}_\Gamma(V - \langle V, n\rangle \cdot n) \\ + \Big(g^M \circ \varphi^{-1} \cdot \det D^\tau \varphi^{-1} - f_\varphi\Big) \cdot \nabla_\Gamma f_\varphi^T V\, \mathrm{d}s. \quad (58)\end{aligned}$$

Here, $\mathcal{D}(f_\varphi)$ is the classical shape derivative of f_φ. The first integral corresponds to the classical shape derivative component $g^{\mathcal{N}}$ of decomposition, eq. (20), acting on normal directions. Next, the second integral acts on tangential directions and therefore corresponds to the parameterization part $g^{\mathcal{T}}$ in eq. (20).

2.4. Normal component: minimal surfaces

For illustration, let us deviate from normalization of the target (cf. eq. (40)) by choosing $f_\varphi = 0$ and $g^M = 1$ for all $\varphi \in \operatorname{Emb}_{\partial M}(M, \mathbb{R}^{n+1})$.

In this situation, the classical shape derivative component of $\mathfrak{D}\mathfrak{J}^\tau(\varphi)$ is given by

$$\langle g_\varphi^{\mathcal{N}}, V\rangle = -\frac{\dim(M)}{2} \cdot \int_{\varphi(M)} \big(\det D^\tau \varphi^{-1}(s)\big)^2 \cdot \kappa(s) \cdot \big\langle V(s), n(s)\big\rangle\, \mathrm{d}s. \quad (59)$$

Since φ are embeddings and M compact, the corresponding Jacobians are bounded and non-vanishing. In our special situation this means that the horizontal component of the pre-shape derivative, eq. (59), is vanishing exactly for shapes with vanishing mean curvature κ. Put differently, the minimal surfaces and their higher dimension analogues are exactly the stationary points for this horizontal component.

Hence, a gradient ascent using eq. (59), resembles an algorithm for evolutionary surfaces, proposed by Dziuk (1990), which solves Plateau's problem by approximating a mean curvature flow. Note that an ascent is necessary, since our formulation of the pre-shape parameterization tracking problem involves inverse Jacobians, which is connected to Plateau's problem by

$$\max_{\varphi\in\mathrm{Emb}_{\partial M}(M,\mathbb{R}^{n+1})} \int_{\varphi(M)} \left(\det D^\tau \varphi^{-1}(s)\right)^2 \,\mathrm{d}s \Leftrightarrow$$

$$\Leftrightarrow \min_{\varphi\in\mathrm{Emb}_{\partial M}(M,\mathbb{R}^{n+1})} \int_M |\det D^\tau \varphi(s)| \,\mathrm{d}s. \tag{60}$$

This also illustrates the qualitative properties of a steepest descent using the complete pre-shape derivative. Briefly stated, if less vertices are desired at a location, the gradient descent in normal direction tends to blow up the shape, increasing distances of neighboring vertices. If more vertices are desired, it tends to locally flatten the shape, driving the nodes together. This shows that application of the full pre-shape derivative distorts the shape in normal direction, hence interfering with the actual shape optimization problem to be regularized.

Use of the tangential component in eq. (56) leads to algorithms similar to the mesh deformation methods from Liao and Anderson (1992), Grajewski, Köster and Turek (2009), and Cao, Huang and Russell (2002). Such a routine is discussed and implemented in the numerical Section 3. We will use it in upcoming works to construct various regularization methods for shape optimization problems.

An illustrative numerical example of a pre-shape derivative for the parameterization tracking problem and its decomposition is shown in Fig. 5 for target $f_\varphi(x,y,z) \equiv \frac{1}{\int_{\varphi(M)} 1 \,\mathrm{d}s} \cdot x$ and a sphere centered at $(0.5, 0.5, 0.5)$.

2.5. A class of externally defined targets f_φ

As we have left the target f_φ unspecified during derivation of the pre-shape derivative, eq. (44), we want to give a constructive example, which can be implemented in numerical routines. To do so, we have to keep in mind that the normalization requirement, eq. (40), on f_φ has to be fulfilled. One way to accomplish this is by defining f_φ using a given globally defined function $q : \mathbb{R}^{n+1} \to (0,\infty)$. By assuming H^2-regularity for q, existence of pre-shape derivatives and their closed form as in eq. (44) is guaranteed. The corresponding

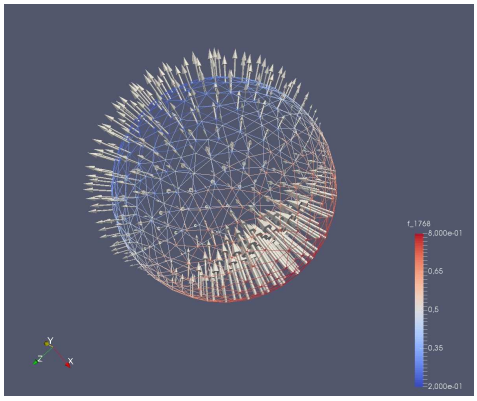

(a) Normal component representing the classical shape part

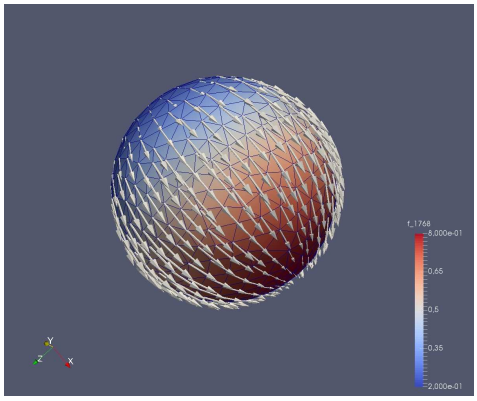

(b) Tangential component representing the parameterization part

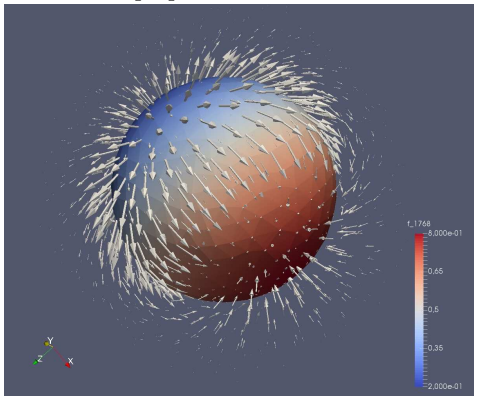

(c) Complete pre-shape gradient in volume mesh representation

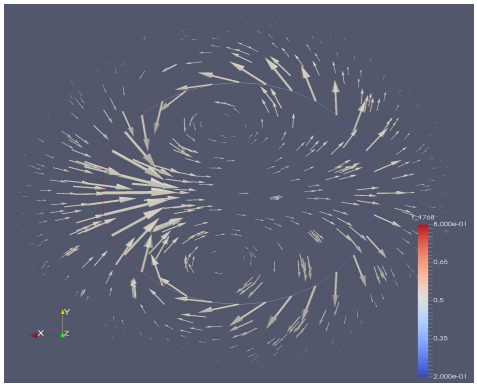

(d) Slice through xy-plane at center of complete volume pre-shape gradient

Figure 5: Negative pre-shape gradient of $\mathfrak{J}^\tau$ on a sphere scaled by 0.02 using target $f_\varphi(x,y,z) \equiv \frac{1}{\int_{\varphi(M)} 1 \,\mathrm{d}s} \cdot x$, which is depicted by color, and gradient representation by a linear elasticity metric. Color shifting towards red means higher desire for more volume/vertex allocation

target vertex density on a shape $\varphi(M)$ is then given by

$$f_\varphi = \frac{\int_M g^M \,\mathrm{d}s}{\int_{\varphi(M)} q_{|\varphi(M)} \,\mathrm{d}s} \cdot q_{|\varphi(M)}, \tag{61}$$

which is well defined due to the trace theorem for Sobolev functions.

If the target f_φ is chosen such that normalization eq. (40) is not fulfilled, solutions to the parameterization tracking problem, eq. (41), might still exist. Depending on whether $\int_M g^M \,\mathrm{d}s$ is greater or smaller than $\int_M f_\varphi \,\mathrm{d}s$, the gra-

dient flow, generated by the pre-shape derivative, eq. (44), locally shrinks or blows up the shape $\varphi(M)$ in normal direction to compensate for the difference.

Next, we calculate $\mathfrak{D}_m(f_\varphi)[V]$, which exists since we have $q_{|\varphi(M)} \in H^1\big(\varphi(M)\big)$. For this, we apply pre-shape calculus rules established in Corollary 2. Also, since the external force $q : \mathbb{R}^{n+1} \to (0,\infty)$ is defined on the entire ambient space, we can make direct use of decomposition for pre-shape material derivatives from Corollary 1. Together with the fact that q and g^M do not depend on φ, this gives

$$\begin{aligned}
\mathfrak{D}_m(f_\varphi)[V] &= \mathfrak{D}_m\left(\frac{\int_M g^M \,\mathrm{d}s}{\int_{\varphi(M)} q \,\mathrm{d}s} \cdot q\right)[V] \\
&= -\frac{\int_M g^M \,\mathrm{d}s}{\big(\int_{\varphi(M)} q \,\mathrm{d}s\big)^2} \cdot q \cdot \int_{\varphi(M)} \big(\mathfrak{D}_m(q)[V] + \mathrm{div}_\Gamma(V) \cdot q\big) \,\mathrm{d}s \\
&\quad + \frac{\int_M g^M \,\mathrm{d}s}{\int_{\varphi(M)} q \,\mathrm{d}s} \cdot \Big(\mathfrak{D}(q)[V] + \nabla q^T V\Big) \\
&= -\frac{\int_M g^M \,\mathrm{d}s}{\big(\int_{\varphi(M)} q \,\mathrm{d}s\big)^2} \cdot q \cdot \int_{\varphi(M)} \Big(\nabla q^T V + \mathrm{div}_\Gamma(V) \cdot q\Big) \,\mathrm{d}s \\
&\quad + \frac{\int_M g^M \,\mathrm{d}s}{\int_{\varphi(M)} q \,\mathrm{d}s} \cdot \nabla q^T V \\
&= -\frac{\int_M g^M \,\mathrm{d}s}{\big(\int_{\varphi(M)} q \,\mathrm{d}s\big)^2} \cdot q \cdot \int_{\varphi(M)} \Big(\frac{\partial q}{\partial n} + \dim(M) \cdot \kappa \cdot q\Big) \cdot \langle V, n\rangle \,\mathrm{d}s \\
&\quad + \frac{\int_M g^M \,\mathrm{d}s}{\int_{\varphi(M)} q \,\mathrm{d}s} \cdot \nabla q^T V,
\end{aligned} \tag{62}$$

where the last equality stems from the Stokes theorem and our assumption on V to vanish on the boundary $\partial\varphi(M)$, and κ denotes the mean curvature as in eq. (55).

Next, we illustrate how the closed pre-shape derivative formula can be used to derive additional important properties of pre-shape optimization problems. In particular, we will see that local and global solutions parameterization tracking in each fiber coincide.

Proposition 3 (Characterization of Global Solutions by Fiber Stationarity) *Let assumptions of Theorem 2 be satisfied. Then the following statements are equivalent:*

(i) $\varphi \in \mathrm{Emb}(M, \mathbb{R}^{n+1})$ *is a fiber stationary point of eq.* (41)*, i.e.*

$$\mathfrak{D}\mathfrak{J}^\tau(\varphi)[V] = 0 \quad \forall V \in C^\infty_{\partial M}(\mathbb{R}^{n+1}, \mathbb{R}^{n+1}) \text{ with } \langle \mathrm{Tr}_{|\,\mathrm{int}\,\varphi(M)}[V], n\rangle_2 = 0, \tag{63}$$

where $\operatorname{int}\varphi(M)$ *is the interior of* $\varphi(M)$ *and* n *is the outer normal field on* $\operatorname{int}\varphi(M)$.

(ii) φ *is a global solution to eq.* (41)*, and, in particular, it satisfies*

$$g^M \circ \varphi^{-1} \cdot \det D^\tau \varphi^{-1} = f_\varphi \quad \text{on } \varphi(M). \tag{64}$$

(iii) the complete pre-shape derivative of $\mathfrak{J}^\tau$ *vanishes in* φ*, i.e.*

$$\mathfrak{D}\mathfrak{J}^\tau(\varphi)[V] = 0 \quad \forall V \in C^\infty_{\partial M}(\mathbb{R}^{n+1}, \mathbb{R}^{n+1}). \tag{65}$$

In particular, its normal component $g^{\mathcal{N}}_\varphi$ *in* φ *vanishes.*

The necessary first order condition regarding only directions V *tangential to* $\varphi(M)$ *is already a sufficient condition for being a global minimizer to* $\mathfrak{J}^\tau$*.*

Proof Let us assume the setting of Theorem 2. We show the equivalence of all assertions by a circular argument '$(i) \implies (ii) \implies (iii) \implies (i)$'.

As a start, implication '$(ii) \implies (iii)$' is trivial. By assuming (ii), we can use relation of eq. (64) to see that the two integrands of $\mathfrak{D}\mathfrak{J}^\tau(\varphi)[V]$ (cf. eq. (44)) featuring $g^M \circ \varphi^{-1} \cdot \det D^\tau \varphi^{-1}$ and f_φ are zero for all directions $V \in C^\infty_{\partial M}(\mathbb{R}^{n+1}, \mathbb{R}^{n+1})$. The same argument applies for the normal component $g^{\mathcal{N}}_\varphi$ by using the explicit decomposition, eq. (56). Hence, we immediately get eq. (65).

The non-trivial part is to prove '$(i) \implies (ii)$'. Let us assume (i) by fixing a $\varphi \in \operatorname{Emb}(M, \mathbb{R}^{n+1})$, satisfying fiber stationarity, eq. (63). With the pre-shape derivative formula from Theorem 2 at hand, we can apply an integration by parts on manifolds (see Taylor, 2011, Chapter 2.2, Proposition 2.3), either using the fact that M is closed or V is vanishing on the boundary, to get

$$\mathfrak{D}\mathfrak{J}^\tau(\varphi)[V] = \int_{\varphi(M)} \left((g^M \circ \varphi^{-1} \cdot \det D^\tau \varphi^{-1}) \cdot \left(\nabla_\Gamma (g^M \circ \varphi^{-1} \cdot \det D^\tau \varphi^{-1}) - \nabla_\Gamma f_\varphi \right) \right)^T V \mathrm{d}s, \tag{66}$$

where we also used the assumption in Proposition 2 that f_φ is constant in each fiber and $\langle \operatorname{Tr}_{|\varphi(M)}[V], n \rangle_2 = 0$ to reformulate $\mathfrak{D}_m(f_\varphi)[V]$. Due to assumption of eq. (63) of fiber stationarity, we know that eq. (66) equals zero for all V tangential on $\varphi(M)$ up to the boundary. So, in the interior of $\varphi(M)$ we get

$$(g^M \circ \varphi^{-1} \cdot \det D^\tau \varphi^{-1}) \cdot \left(\nabla_\Gamma \big(g^M \circ \varphi^{-1} \cdot \det D^\tau \varphi^{-1} \big) - \nabla_\Gamma f_\varphi \right) \equiv 0. \tag{67}$$

By assumption, we have $g^M > 0$, so, together with the non-vanishing determinant by $\varphi \in \operatorname{Emb}(M, \mathbb{R}^{n+1})$, this implies

$$\nabla_\Gamma (g^M \circ \varphi^{-1} \cdot \det D^\tau \varphi^{-1} - f_\varphi) \equiv 0. \tag{68}$$

Since the involved functions are Lipschitz continuous, and as Proposition 3 assumes M to be smooth and path connected, we can derive constancy of the

involved term. However, after using a pull-back and normalization assumption, eq. (40), we see that the discussed constant is 0, giving us

$$g^M \circ \varphi^{-1} \cdot \det D^\tau(\varphi)^{-1} = f_\varphi \text{ on } \varphi(M). \tag{69}$$

Since φ is chosen from $\mathrm{Emb}_{\partial M}(M, \mathbb{R}^{n+1})$, it leaves the boundary fixed, finally giving '$(i) \implies (ii)$'.

Lastly, we easily see that '$(iii) \implies (i)$'. Since the complete vanishing of the pre-shape derivative, eq. (65), implies, in particular, its vanishing for directions V tangential to $\varphi(M)$, which is eq. (63), and this concludes the proof. □

Proposition 3 tells us that there are no stationary points other than global solutions to the pre-shape parameterization tracking problem, eq. (41). This strongly resembles the situation for convex optimization problems, where the only candidates for local optimality are indeed global solutions.

Notice that Proposition 3 gives the existence of stationary points φ for each shape. Since stationary points are global solutions, we can simply use the existence result of Proposition 2 for this.

Additionally, Proposition 3 guarantees that optimization with the tangential component of pre-shape derivative eq. (44) is sufficient for reaching a globally optimal solution for (41). This permits the design of regularizations for shape optimization algorithms using pre-shape parameterization tracking with the property to leave the shape at hand invariant, while at the same time finding an optimal parameterization of the respective shape.

3. Numerical tests of parameterization tracking involving pre-shape derivatives

We have now finished our introduction of pre-shape calculus and its application to parameterization tracking problems. In order to test our theoretical results, we present three implementations of pre-shape gradient descent methods for the parameterization tracking problem. For this we use the open-source finite-element software FEniCS (see Logg et al., 2012; Alnaes et al., 2015). Construction of meshes is done via the free meshing software Gmsh (see Geuzaine and Remacle, 2007). We use a single core of an Intel(R) Core(Tm) i3-8100 CPU at 3.60 GHz featuring 16 GB RAM. The single core runs at 800 MHz while the code is executed on a virtual machine.

In the following, we show three implementations solving the parameterization tracking problem, eq. (41), by using the tangential component of the pre-shape derivative seen in decomposition, eq. (56). The solution process also features a simple backtracking line search, which scales the initial gradient of the current iteration U_i according to a given factor c and rescales it by 0.5 if no sufficient decrease in $\mathfrak{J}$ is apparent. In order to apply a descent algorithm, we are in need of pre-shape gradients. Because gradients are defined with respect

to a sufficient bilinear form, we have to choose a form which fits our application. Since we are in infinite dimensions, there is a multitude of non-equivalent choices to represent derivatives as gradients. These can differ in resulting regularity of the gradients, and also in computational expense. As a bilinear form, we choose the weak formulation of the linear elasticity as proposed in Schulz, Siebenborn and Welker (2016), which gives us H^1-regularity of pre-shape gradients. By only using the shear component of the linear elasticity, featuring the second Lamé parameter μ_{elas}, and adding a zero order term, the gradient U is calculated by solving its representing system

$$\begin{aligned}
\alpha_{\text{LE}} \cdot \int_{\mathbb{D}} \mu_{\text{elas}} \cdot \epsilon(U) : \epsilon(V) \, \mathrm{d}x + \alpha_{L^2} \cdot (U,V)_{L^2(\mathbb{D})} &= \mathfrak{D}\mathfrak{J}^\tau(\varphi)[V] \\
&\forall V \in H_0^1(\mathbb{D}, \mathbb{R}^{n+1}) \\
&\epsilon(U) = \frac{1}{2}(\nabla U^T + \nabla U) \\
&\epsilon(V) = \frac{1}{2}(\nabla V^T + \nabla V) \\
&U = 0 \qquad \text{on } \partial\mathbb{D}.
\end{aligned} \tag{70}$$

Here, we choose the weights $\alpha_{\text{LE}}, \alpha_{L^2} > 0$. For $\mu_{\max}, \mu_{\min} > 0$, the second Lamé parameter μ_{elas} is chosen as the solution of the Poisson problem

$$\begin{aligned}
-\Delta \mu_{\text{elas}} &= 0 && \text{in } \mathbb{D} \\
\mu_{\text{elas}} &= \mu_{\max} && \text{on } \varphi(M) \\
\mu_{\text{elas}} &= \mu_{\min} && \text{on } \partial\mathbb{D}.
\end{aligned} \tag{71}$$

Solving eq. (70) on the entire hold-all domain $\mathbb{D}$ gives us a volume representation U of the pre-shape derivative $\mathfrak{D}\mathfrak{J}^\tau$. The pre-shape gradient system of eq. (70) is assembled in FEniCS and solved with a sparse LU method from PETSc used as a linear algebra backend.

The first example shows an application of the parameterization tracking problem for improving the quality of a given hold-all domain $\mathbb{D} = [0,1]^2 \subset \mathbb{R}^2$. This is realized by using an unstructured 2-dimensional volume mesh created via Gmsh, featuring 4262 triangular cells and 2212 nodes. Then we distort the mesh quality of this unstructured mesh by applying

$$\varphi_0 \begin{pmatrix} x \\ y \end{pmatrix} = \begin{pmatrix} 0.025 \cdot \sin(25.5 \cdot x) \\ 0 \end{pmatrix} \tag{72}$$

as a deformation to the interior of $\mathbb{D}$. The deformed initial mesh $\varphi_0(\mathbb{D})$ is depicted in Fig. 6 (a). Notice that in this scenario the initial model M is given by the hold-all domain $\mathbb{D} = [0,1]^2$ with non-trivial boundary $\partial\mathbb{D}$. Therefore, we are in the situation, where the boundary $\partial\mathbb{D}$ is left invariant (cf. eq. (39)). Also, there is no normal component of the pre-shape derivative in this case, as the codimension of $\mathbb{D} \subset \mathbb{R}^2$ is zero.

To formulate the parameterization tracking problem of eq. (41), we need to specify an initial point distribution g^M and target f_φ. Here, the target chosen is given by the constant

$$f_\varphi \equiv \frac{1}{\int_{\mathbb{D}} 1 \, \mathrm{d}x}. \tag{73}$$

This ensures that a uniform cell volume distribution of the hold-all domain is targeted. The initial point distribution g^M is represented by using a continuous Galerkin Ansatz with linear elements. Degrees of freedom are situated at the mesh vertices and set to the average of inverses of surrounding cell volumes, i.e.

$$g^M(p_i) = \frac{1}{|\mathcal{C}_i|} \cdot \sum_{C \in \mathcal{C}_i} \frac{1}{\int_C 1 \, \mathrm{d}x}. \tag{74}$$

Here p_i is a mesh vertex and $\mathcal{C}_i$ is the set of its neighboring cells C. Finally, the resulting function is normed to satisfy the demanded normalization condition, eq. (40), of the parameterization tracking problem. The initial point distribution estimated by this procedure is shown in Fig. 6 (a).

With both g^M and f_φ specified, the target $\mathfrak{J}^\tau$ and its pre-shape derivative $\mathfrak{D}\mathfrak{J}^\tau$ can be assembled. For the gradient representation we use weights $\alpha_{\mathrm{LE}} = 0.02$, $\alpha_{L^2} = 1$ and Lamé parameters $\mu_{\max} = \mu_{\min} = 1$, resulting in constant $\mu_{\mathrm{elas}} = 1$. An initial scaling factor of $c = 0.01$ for the negative gradient during line search is applied. The method successfully exits after 37.07s and 45 iterations. Results of the pre-shape gradient descent using the tangential component of the pre-shape derivative and the described methodology are shown in Figs. 6 and 8.

For our second example, we use the exactly same parameters as in the first example. Note that, in particular, the starting mesh and therefore its initial volume distribution g^M are the same as in the first example. We can see an illustration in Fig. 6 (a). To show the general applicability of parameterization tracking, we replace the uniform target f_φ from eq. (73) by a more complicated non-uniform target

$$f_\varphi = \frac{\int_{[0,1]} \int_{[0,1]} g^M(x,y) \, \mathrm{d}x \, \mathrm{d}y}{\int_{[0,1]} \int_{[0,1]} 2 + \cos\left(5 \cdot 2\pi \cdot \left((x-0.35)^2 + 2 \cdot (y-0.4)^2\right)\right) \mathrm{d}x \, \mathrm{d}y} \cdot \\ \cdot \left(2 + \cos\left(5 \cdot 2\pi \cdot \left((x-0.35)^2 + 2 \cdot (y-0.4)^2\right)\right)\right). \tag{75}$$

The pre-shape gradient descent for this non-uniform target achieves convergence after 38.12 s and 46 iterations. We visualize an intermediate mesh, and the final mesh in Figs. 6 (c) and (d). The target function values $\mathfrak{J}^\tau(\varphi_i)$ and pre-shape gradient norms are shown in Fig. 8. Interestingly, notice that the intermediate mesh (c) looks like a superposition of the final and initial meshes (d) and (a).

Essentially, this is an illustration of snapshots from a discretized flow in the fiber of $\mathrm{Emb}(\mathbb{D},\mathbb{D})$, corresponding to the shape $\mathbb{D}$, which is abstractly visualized in Fig. 2. We see in Fig. 6 (d) that the prescribed non-uniform cell volume distribution is achieved, even though the initial mesh in Fig. 6 (d) has degenerate cells distributed on vertical lines.

Our third example applies the parameterization tracking problem to a sphere centered in the hold-all domain $\mathbb{D} = [0,1]^3 \subset \mathbb{R}^3$. It acts as the modeling manifold M and its initial parameterization φ_0 is given by the identity embedding it into the hold-all domain. The initial shape is a structured triangular surface mesh, approximating a sphere centered in $(0.5, 0.5, 0.5)$ with radius 0.3 using Gmsh. It consists of 6 240 triangular cells and 3 122 vertices on the surface. The sphere is embedded in a hold-all domain consisting of 21 838 tetraedic cells and 4 059 nodes.

For the third example we target a non-uniform surface cell volume distribution given by

$$f_\varphi \begin{pmatrix} x \\ y \\ z \end{pmatrix} = \frac{1}{\int_{\varphi(M)} 1 + \frac{1}{2} \cdot \sin(10 \cdot 2\pi \cdot x) \,\mathrm{d}s} \cdot \big(1 + \frac{1}{2} \cdot \sin(10 \cdot 2\pi \cdot x)\big). \quad (76)$$

The target function is of the form of eq. (61), which permits the use of the material derivative formula of eq. (62) for assembling the pre-shape derivative $\mathfrak{D}\mathfrak{J}^\tau$. At the same time, it satisfies the normalization condition of eq. (40). Also, we set the initial vertex distribution to a constant

$$g^M \equiv \frac{1}{\int_M 1 \,\mathrm{d}s}. \quad (77)$$

In order to calculate covariant derivatives and associated Jacobian determinants, we apply a Gram-Schmidt algorithm to construct local tangential orthonormal bases. Here, we choose weights $\alpha_{\mathrm{LE}} = 0.02$, $\alpha_{L^2} = 1$ and Lamé parameters $\mu_{\max} = 30$, $\mu_{\min} = 5$ for gradient representation. The line search employs an initial scaling factor $c = 0.001$ for the negative gradient. For this scenario, the gradient representation of the pre-shape derivative, and the resulting surface mesh with its associated vertex distribution are depicted in Fig. 7. The method successfully exits after 1256.78 s and 48 iterations. Target function values $\mathfrak{J}^\tau(\varphi_i)$ and pre-shape gradient norms are shown in Fig. 8. In the light of Proposition 3, we see that the gradient norm and target values converge simultaneously by using tangential components of $\mathfrak{D}\mathfrak{J}^\tau$ only. Also, the shape of the sphere is left invariant, which would not be the case if normal components or the full pre-shape derivative (cf. Fig. 5) were used.

4. Conclusion and outlook

In this work we introduced a unified framework to formulate shape optimization and mesh quality optimization problems. A calculus for pre-shape derivatives,

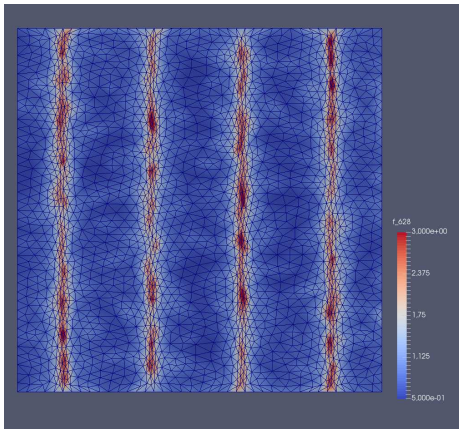

(a) Initial mesh $\varphi_0(M)$

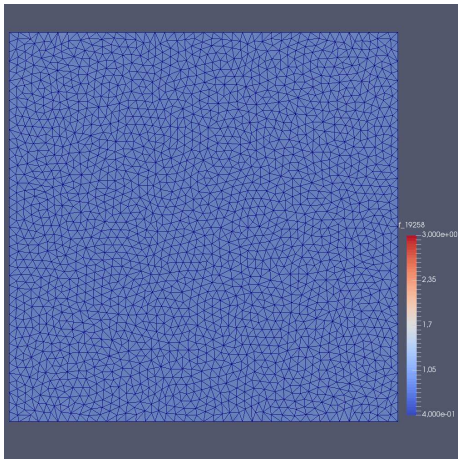

(b) Final mesh $\varphi_{45}(M)$ for uniform target

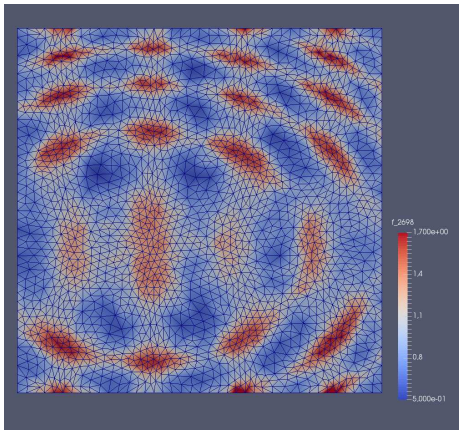

(c) Intermediate mesh $\varphi_6(M)$ for non-uniform target

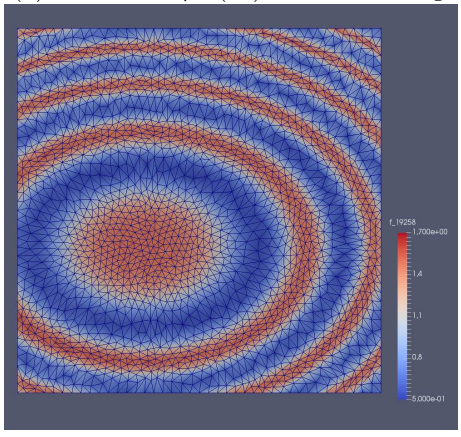

(d) Final mesh $\varphi_{46}(M)$ for non-uniform target

Figure 6: (a) Initial point distribution g^M depicted by color on the distorted initial mesh $\varphi_0(M)$.
(b) Final mesh $\varphi_{45}(M)$ for the uniform target after 45 pre-shape gradient descent iterations with associated point distribution $g^M \circ \varphi_{45}^{-1} \cdot \det D\varphi_{45}^{-1}$ shown in color.
(c) Intermediate mesh $\varphi_6(M)$ for the non-uniform target after 6 pre-shape gradient descent iterations with associated point distribution $g^M \circ \varphi_6^{-1} \cdot \det D\varphi_6^{-1}$ shown in color.
(d) Final mesh $\varphi_{46}(M)$ for the non-uniform target after 46 pre-shape gradient descent iterations with associated point distribution $g^M \circ \varphi_{46}^{-1} \cdot \det D\varphi_{46}^{-1}$ shown in color.

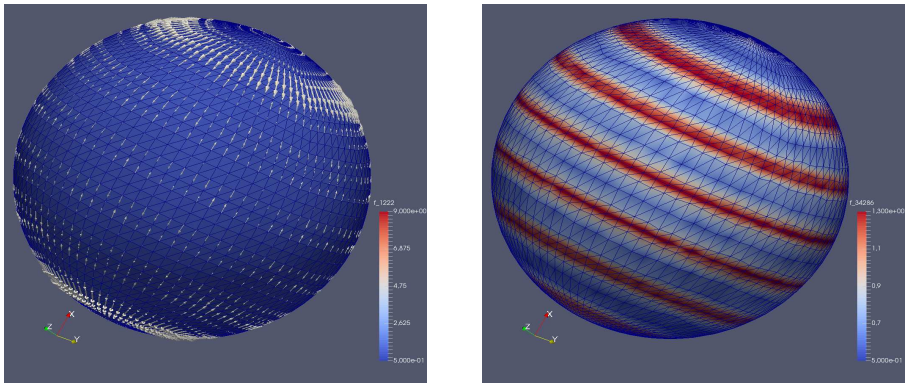

(a) g^M and $-U$ on $\varphi_0(M)$ (b) $g^M \circ \varphi_{48}^{-1} \cdot \det D\varphi_{48}^{-1}$ on $\varphi_{48}(M)$

Figure 7: (a) Constant initial point distribution g^M and negative pre-shape derivative $-\mathfrak{D}\mathfrak{J}^\tau(\varphi_0)$ represented via eq. (70) on the initial surface mesh $\varphi_0(M)$ scaled by 0.03.
(b) Resulting surface mesh $\varphi_{48}(M)$ after 48 pre-shape gradient descent iterations with associated point distribution $g^M \circ \varphi_{48}^{-1} \cdot \det D\varphi_{48}^{-1}$ shown in color

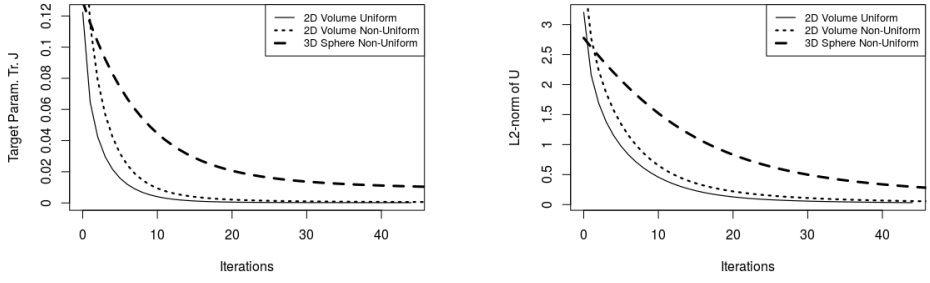

(a) $\mathfrak{J}^\tau(\varphi_i)$ (b) $\|U_i\|_{L^2(\mathbb{D},\mathbb{R}^{n+1})}$

Figure 8: (a) Values for the pre-shape parameterization tracking target $\mathfrak{J}^\tau(\varphi_i)$ for iterates φ_i of the tangential pre-shape derivative component based steepest descent method. Target for the 3D sphere case is scaled by 3.
(b) L^2-norms $\|U_i\|_{L^2(\mathbb{D},\mathbb{R}^{n+1})}$ of the gradient representations U_i of pre-shape derivatives for each iterate φ_i. Gradient norms for the 3D sphere case are scaled by 25

which act in normal and tangential directions, and the corresponding structure theorems were derived. In particular, rules and problem formulations from classical shape optimization carry over to the pre-shape setting. These techniques were tested on a class of parameterization tracking problems. Resulting nu-

merical implementations of a gradient descent method, based on decomposed pre-shape derivatives, show promising results for optimization of volume- and surface mesh quality.

In forthcoming works we will derive efficient algorithms harnessing the opportunity of simultaneously solving shape optimization problems and improving mesh quality of shapes and ambient spaces. For this, we will design various targets for parameterization tracking, giving a desired type of mesh for the user. Also, we will define pre-shape Hessians to harness second order information. (Quasi-)Newton methods in the context of pre-shape optimization, as well as an optimal choice of pre-shape gradient representations, will enhance the performance of these algorithms.

Acknowledgements

The authors would like to thank Leonhard Frerick (Trier University) and Jochen Wengenroth (Trier University) for a helpful and interesting discussion about differentiability in infinite dimensions. This work has been supported by the BMBF (Bundesministerium für Bildung und Forschung) within the collaborative project GIVEN (FKZ: 05M18UTA). Further, the authors acknowledge the support of the DFG research training group 2126 on algorithmic optimization.

References

Algorri, M.E. and Schmitt, F. (1996) Mesh Simplification. In: *Computer Graphics Forum*, 15, 77–86. Wiley Online Library.

Alnæs, M.S., Blechta, J., Hake, J., Johansson, A., Kehlet, B., Logg, A., Richardson, C., Ring, J., Rognes, M.E. and Wells, G.N. (2015) The FEniCS project version 1.5. *Archive of Numerical Software*, **3**(100).

Banyaga, A. (1974) Formes-volume sur les variétés a bord. *Enseignement Math*, **20**(2): 127–131.

Bauer, M., Bruveris, M. and Michor, P.W. (2014) Overview of the Geometries of Shape Spaces and Diffeomorphism Groups. *Journal of Mathematical Imaging and Vision*, **50**(1-2): 60–97.

Berggren, M. (2010) A Unified Discrete–Continuous Sensitivity Analysis Method for Shape Optimization. In: *Applied and Numerical Partial Differential Equations*, *Computational Methods in Applied Sciences*, **15**, 25–39. Springer.

Binz, E. and Fischer, H.R. (1981) The manifold of embeddings of a closed manifold. In: *Differential Geometric Methods in Mathematical Physics*, 310–325. Springer.

Bochev, P., Liao, G. and dela Pena, G.(1996) Analysis and Computation of Adaptive Moving Grids by Deformation. *Numerical Methods for Partial Differential Equations: An International Journal*, **12**(4): 489–506.

Cai, X., Jiang, B. and Liao, G. (2004) Adaptive Grid Generation Based on the Least-Squares Finite-Element Method. *Computers & Mathematics with Applications*, **48**(7-8): 1077–1085.

Cao, W., Huang, W. and Russell, R.D. (1999) A Study of Monitor Functions for Two-Dimensional Adaptive Mesh Generation. *SIAM Journal on Scientific Computing*, **20**(6): 1978–1994.

Cao, W., Huang, W. and Russell, R.D. (2002) A Moving Mesh Method Based on the Geometric Conservation Law. *SIAM Journal on Scientific Computing*, **24**(1): 118–142.

Dacorogna, B. and Moser, J. (1990) On a Partial Differential Equation Involving the Jacobian Determinant. In: *Annales de l'Institut Henri Poincare (C) Non Linear Analysis*, **7**, 1–26. Elsevier.

Delfour, M.C. and Zolésio, J.-P. (2001) *Shapes and Geometries: Metrics, Analysis, Differential Calculus, and Optimization*, *Advances in Design and Control*, **22**. SIAM, 2nd edition.

Dziuk, G. (1990) An Algorithm for Evolutionary Surfaces. *Numerische Mathematik*, **58**(1): 603–611.

Dziuk, G. and Hutchinson, J. (1999) The Discrete Plateau Problem: Algorithm and Numerics. *Mathematics of Computation*, **68**(225): 1–23.

Ebin, D.G. and Marsden, J. (1970) Groups of Diffeomorphisms and the Motion of an Incompressible Fluid. *Ann. Math.*, **92**(1): 102–163.

Etling, T., Herzog, R., Loayza, E. and Wachsmuth, G. (2018) First and second order shape optimization based on restricted mesh deformations. *arXiv preprint arXiv:1810.10313*.

Field, D.A. (1988) Laplacian Smoothing and Delaunay Triangulations. *Communications in Applied Numerical Methods*, **4**(6): 709–712.

Freitag, L.A. (1997) On combining Laplacian and optimization-based mesh smoothing techniques. Technical report, Argonne National Lab., IL (United States).

Frey, P.J. and Borouchaki, H. (1999) Surface Mesh Quality Evaluation. *International Journal for Numerical Methods in Engineering*, **45**(1): 101–118.

Geuzaine, C. and Remacle, J.-F. (2007) Gmsh: A Three-Dimensional Finite Element Mesh Generator with Built-In Pre-and Post-Processing Facilities. In *Proceedings of the Second Workshop on Grid Generation for Numerical Computations, Tetrahedron II*.

Grajewski, M., Köster, M. and Turek, S. (2009) Mathematical and Numerical Analysis of a Robust and Efficient Grid Deformation Method in the Finite Element Context. *SIAM Journal on Scientific Computing*, **31**(2): 1539–1557.

Grajewski, M., Köster, M. and Turek, S. (2010) Numerical Analysis and Implementational Aspects of a New Multilevel Grid Deformation Method. *Applied Numerical Mathematics*, **60**(8): 767–781.

Haslinger, J. and Mäkinen, R.A.E. (2003) *Introduction to Shape Optimization: Theory, Approximation, and Computation. Advances in Design and Control*, **7**. SIAM.

Henrot, A. and Pierre, M. (2018) *Shape Variation and Optimization. Tracts in Mathematics*, **7**. European Mathematical Society.

Johnston, B.P., Sullivan Jr, J.M. and Kwasnik, A. (1991) Automatic Conversion of Triangular Finite Element Meshes to Quadrilateral Elements. *International Journal for Numerical Methods in Engineering*, **31**(1): 67–84.

Kendall, D.G., Barden, D., Carne, T.K. and Le, H. (2009) *Shape and Shape Theory. Wiley Series in Probability and Statistics*, **500**. John Wiley & Sons.

Kriegl, A. and Michor, P.W. (1997) *The Convenient Setting of Global Analysis. Mathematical Surveys and Monographs*, **53**. American Mathematical Society.

Laurain, A. and Walker, S. (2020) Optimal Control of Volume-Preserving Mean Curvature Flow. *Journal of Computational Physics*, 483: 110373, 2021.

Lee, J.M. (2009) *Manifolds and Differential Geometry. Graduate Studies in Mathematics*, **107**. American Mathematical Society.

Lee, J.M. (2013) *Introduction to Smooth Manifolds*. Springer.

Liao, G. and Anderson, D. (1992) A New Approach to Grid Generation. *Applicable Analysis*, **44**(3-4): 285–298.

Liu, F., Ji, S. and Liao, G. (1998) An Adaptive Grid Method and its Application to Steady Euler Flow Calculations. *SIAM Journal on Scientific Computing*, **20**(3): 811–825.

Logg, A., Mardal, K.-A., Wells, G.N. et al. (2012) *Automated Solution of Differential Equations by the Finite Element Method*. Springer.

Luft, D. and Schulz, V. (2021) Simultaneous Shape and Mesh Quality Optimization using Pre-Shape Calculus. *Control and Cybernetics*, **50**(4).

Michor, P.W. and Mumford, D. (2007) Overview of the Geometries of Shape Spaces and Diffeomorphism Groups. *Applied and Computational Harmonic Analysis*, **23**(1): 74–113.

Moser, J. (1965) On the Volume Elements on a Manifold. *Transactions of the American Mathematical Society*, **120**(2): 286–294.

Onyshkevych, S. and Siebenborn, M. (2020) Mesh Quality Preserving Shape Optimization using Nonlinear Extension Operators. *arXiv preprint arXiv:2006.04420*.

Pinkall, U. and Polthier, K. (1993) Computing Discrete Minimal Surfaces and their Conjugates. *Experimental Mathematics*, **2**(1): 15–36.

Michor, P.W. and Mumford, D. (2005) Vanishing Geodesic Distance on Spaces of Submanifolds and Diffeomorphisms. *Documenta Mathematica*, **10**: 217–245.

Rudin, W. (1991) *Functional Analysis Internat. Ser. Pure Appl. Math.* McGraw-Hill, Inc., 2^{nd} edition.

Schmidt, S. (2014) A Two Stage CVT/Eikonal Convection Mesh Deformation Approach for Large Nodal Deformations. *arXiv preprint arXiv:1411.7663*.

Schulz, V. (2014) A Riemannian View on Shape Optimization. *Foundations of Computational Mathematics*, **14**(3): 483–501.

Schulz, V., Siebenborn, M. and Welker, K. (2016) Efficient PDE Constrained Shape Optimization based on Steklov-Poincaré Type Metrics. *SIAM Journal on Optimization*, **26**(4): 2800–2819.

Shontz, S.M. and Vavasis, S.A. (2003) A Mesh Warping Algorithm Based on Weighted Laplacian Smoothing. In: J. Shepherd, ed., *Proceedings of the 12th International Meshing Roundtable, IMR 2003, Santa Fe, Mew Mexico, USA, September 14-17, 2003*, 147–158.

Smolentsev, N.K. (2007) Diffeomorphism groups of compact manifolds. *Journal of Mathematical Sciences*, **146**(6): 6213–6312.

Sturm, K. (2016) A Structure Theorem for Shape Functions defined on Submanifolds. *arXiv preprint arXiv:1604.04840*.

Taylor, M. (2011) *Partial Differential Equations I: Basic Theory. Applied Mathematical Sciences*, **115**. Springer Science & Business Media, 2nd edition.

Wan, D. and Turek, S. (2006) Numerical Simulation of Coupled Fluid-Solid Systems by Fictitious Boundary and Grid Deformation Methods. In: *Numerical Mathematics and Advanced Applications*, 906–914. Springer.

Welker, K. (2021) Suitable Spaces for Shape Optimization. *Applied Mathematics & Optimization*, 84, 869–902.

Zhang, Y., Bajaj, C. and Xu, G. (2009) Surface Smoothing and Quality Improvement of Quadrilateral/Hexahedral Meshes with Geometric Flow. *Communications in Numerical Methods in Engineering*, **25**(1): 1–18.

Zhou, Z., Chen, X. and Liao, G. (2017) A Novel Deformation Method for Higher Order Mesh Generation. *arXiv preprint arXiv:1710.00291*.